

ZoomEarth: Active Perception for Ultra-High-Resolution Geospatial Vision-Language Tasks

Ruixun Liu^{1*}, Bowen Fu^{1*}, Jiayi Song¹, Kaiyu Li¹, Wanchen Li¹, Lanxuan Xue¹, Hui Qiao², Weizhan Zhang¹, Deyu Meng¹, Xiangyong Cao^{1†}

¹Xi'an Jiaotong University ² China Telecom Shaanxi Branch

Project: <https://earth-insights.github.io/ZoomEarth>

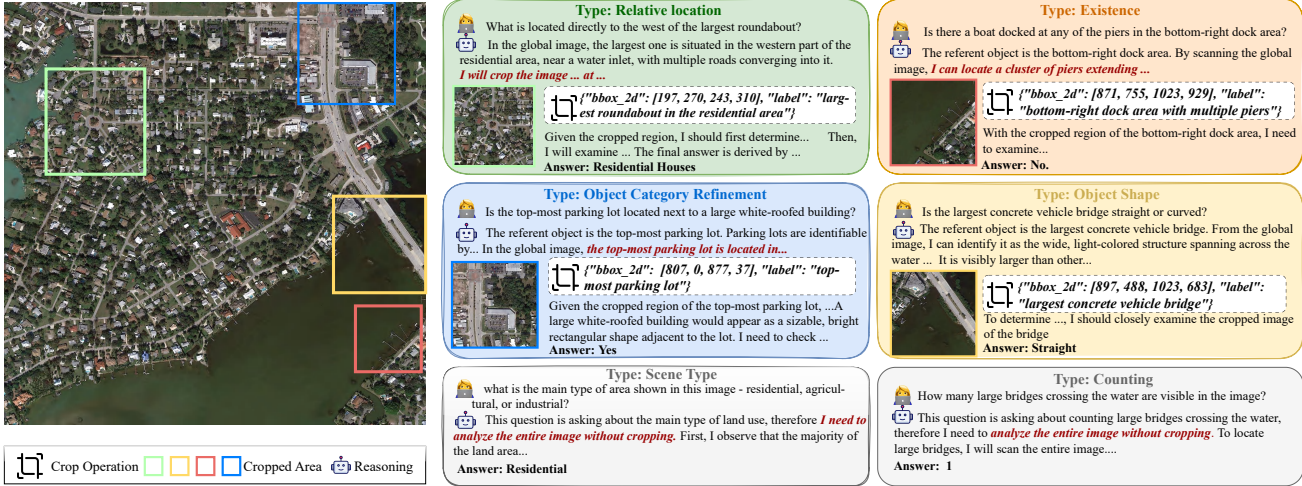


Figure 1. Typical examples from our proposed benchmark LRS-GRO and results obtained by our ZoomEarth framework. LRS-GRO focuses on UHR RS imagery, including 17 multimodal vision-language understanding categories and emphasizing active perception process.

Abstract

Ultra-high-resolution (UHR) remote sensing (RS) images offer rich fine-grained information but also present challenges in effective processing. Existing dynamic resolution and token pruning methods are constrained by a passive perception paradigm, suffering from increased redundancy when obtaining finer visual inputs. In this work, we explore a new active perception paradigm that enables models to revisit information-rich regions. First, we present LRS-GRO, a large-scale benchmark dataset tailored for active perception in UHR RS processing, encompassing 17 question types across global, region, and object levels, annotated via a semi-automatic pipeline. Building on LRS-GRO, we propose ZoomEarth, an adaptive cropping-zooming framework with a novel Region-Guided reward that provides fine-grained guidance. Trained via supervised fine-tuning (SFT) and Group Relative Policy Optimization (GRPO), ZoomEarth achieves state-of-the-art performance on LRS-GRO and, in the zero-shot setting, on three public UHR re-

mote sensing benchmarks. Furthermore, ZoomEarth can be seamlessly integrated with downstream models for tasks such as cloud removal, denoising, segmentation, and image editing through simple tool interfaces, demonstrating strong versatility and extensibility.

1. Introduction

Multimodal large language models (MLLMs) [5, 34, 36, 52] have been developing rapidly, demonstrating remarkable capabilities in multimodal understanding and perception. Several studies [18, 23, 42, 60] have further explored and applied vision-language models (VLMs) to RS images, achieving notable results in tasks such as visual question answering (VQA), grounding, and segmentation. However, satellite and aerial images often cover vast geographic areas, presenting significant challenges in efficiently inputting and processing UHR RS data.

To address this, dynamic-resolution-based methods [24, 35, 58, 71] are developed, enabling models to process high-resolution inputs directly but introduce significant computational cost. Token pruning methods [41, 54] enhance this

*Equal contribution

†Corresponding author (caoxiangyong@mail.xjtu.edu.cn)

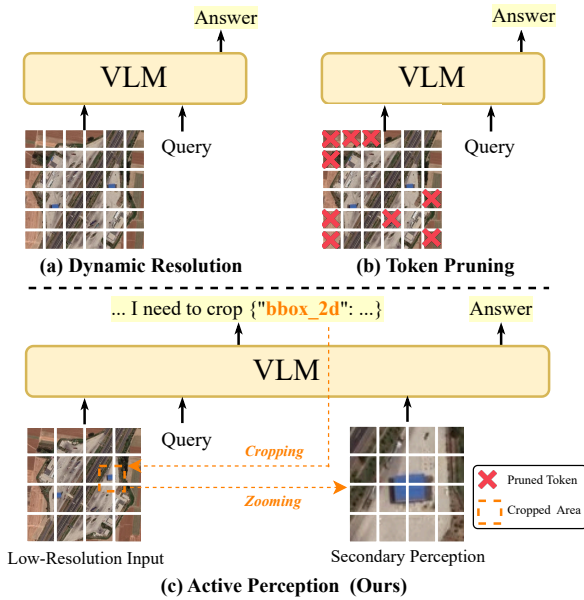


Figure 2. Comparison between passive perception and active perception. (a) Dynamic Resolution [8, 69] and (b) Token Pruning [2, 10] represent passive perception approaches with only a single image input. (c) We introduce a cropping–zooming based active perception method. “Zooming” refers to restoring the cropped image at its original high-resolution image.

process via manually crafted rules (*e.g.*, removing background tokens through clustering), yet they often fail to generalize to RS images with complex backgrounds. As shown in Fig. 2, these studies remain constrained to a passive perception paradigm that relies solely on a single visual input. Specifically, when attempting to acquire more fine-grained visual representations, the model requires higher-resolution image inputs, which in turn forces it to cope with redundant visual information interference.

In this work, to overcome the limitation introduced by passive perception, we explore a new active perception paradigm that enables models to revisit regions relevant to the given query. However, implementing active perception in UHR RS faces two key challenges: (1) the lack of RS image datasets that explicitly capture the active perception process, and (2) the difficulty of enabling models to perform adaptive region selection and active exploration. Recent studies [17, 57] mainly rely on optical character recognition (OCR) and object detection to construct supervised datasets, thereby achieving active perception through tool invocation. However, such approaches are not applicable to the RS domain, which typically lacks textual cues, and features targets that are often expansive regions (*i.e.*, the industrial zone) rather than solely discrete object instances.

To stimulate and enhance active perception in RS, we first present LRS-GRO, a large-scale benchmark dataset tailored for this paradigm. To explicitly model and supervise the active search process, the detail-oriented questions

in LRS-GRO are annotated with precise bounding boxes (BBoxes) for the regions of interest (ROIs). In addition, for the supervised fine-tuning (SFT) dataset, each sample is accompanied by a Chain-of-Thought (CoT) that guides the model to first localize the ROI and then reason about the cropped details. To ensure the fidelity of these annotations, we introduce a novel semi-automatic annotation pipeline, which overcomes the defects observed in automated GPT-based workflows [41] on UHR RS images. Leveraging this pipeline, LRS-GRO encompasses 17 question types across global, region, and object levels, providing a comprehensive benchmark that evaluates not only VQA accuracy but also the active localization of correct ROIs.

Building on this foundation, we propose ZoomEarth, an adaptive cropping–zooming MLLM framework designed for active perception in UHR RS. The model first processes a downsampled global image to gain a holistic understanding. It then actively identifies ROIs, represented as BBoxes. These ROIs are subsequently cropped from the original high-resolution image and re-fed into the model for a detailed perception. As shown in Fig. 1, ZoomEarth can answer global queries from the initial view while adaptively “zooming-in” to handle region and object-specific queries.

The framework is trained using a two-stage strategy as shown in Fig. 3. First, SFT process teaches the model the basic localization-cropping-answering thought pattern. Second, we employ GRPO [46] to enhance its reasoning capabilities. Recognizing that standard IoU-based rewards are often too sparse for UHR images, we introduce a novel Region-Guided reward. This reward leverages the spatial distribution characteristics of RS scenes, providing denser and more fine-grained guidance by rewarding predictions based on their distance to the Ground Truth (GT).

Our main contributions are summarized as follows:

- We propose a UHR RS benchmark dataset, LRS-GRO, which encompasses multi-level question annotations and introduces an evaluation of active perception capabilities.
- We introduce ZoomEarth, a novel active perception framework that adaptively uses the cropping–zooming tool, and propose a Region-Guided reward tailored to the unique spatial properties of RS images.
- Our method achieves state-of-the-art (SOTA) on LRS-GRO and three public UHR RS datasets. Furthermore, it demonstrates strong potential as a foundation model for UHR RS agents, integrating with downstream tasks like cloud removal, segmentation, and image editing in a training-free setting.

2. Related Work

2.1. High-Resolution Image Understanding

High-resolution image understanding persists one of the key challenges for Large Vision-Language Models

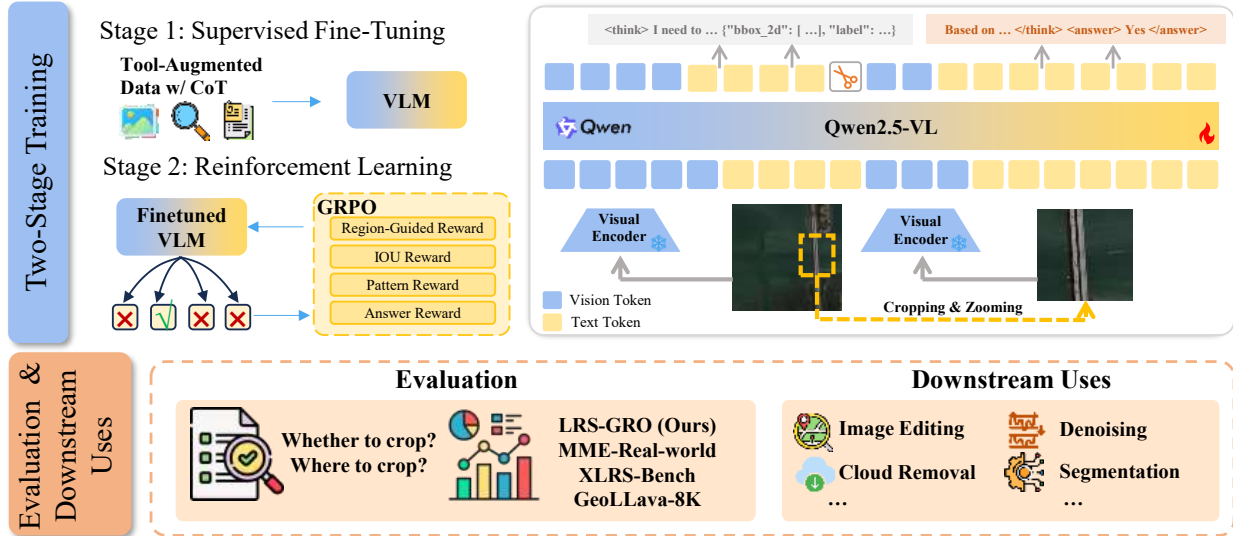


Figure 3. The visualization of the training and evaluation pipeline of our proposed methods. The model architecture diagram in the upper-right corner demonstrates the model’s ability to adaptively crop the ROI by generating the BBox, and subsequently perform advanced reasoning. For clarity in the illustration, we omit the input of query tokens.

(LVLMs) [21, 30, 48]. Some studies on LVLMs [18, 66] propose using positional embedding interpolation to increase input resolution. However, when the input image size is further enlarged, the risk of excessive downsampling remains. Recently, advanced models have introduced dynamic-resolution strategies [4, 7, 32, 62], enabling native understanding of high-resolution images. Nevertheless, such approaches impose additional processing overhead and are susceptible to redundant visual information [20, 67]. In UHR RS imagery, small objects are significantly more numerous and densely distributed [50, 64], further highlighting this challenge. Some studies [11, 31, 40] attempt to introduce separate pathways to preprocess high-resolution image features. LRS-VQA [41] employs a Dynamic Image Pyramid to progressively crop local ROIs based on attention maps. GeoLLava-8k [9] adopts an adaptive token clustering strategy to remove background tokens. However, these models rely on manually predefined external rules and can effectively reduce redundant visual tokens only in specific scenarios (*e.g.*, bridge inspection with large waterbody backgrounds [26]), thereby lacking applicability in diverse VQA contexts. In this paper, we introduce the concept of active perception, enabling the VLM to obtain global context from entire RS imagery and autonomously acquire fine-grained local features, thereby enhancing its comprehension accuracy and reasoning efficiency.

2.2. Visual Reasoning through COT

With the widespread application of CoT [6, 14, 28], VLMs have enhanced their visual perception abilities through reasoning, such as grounding tasks in images [38, 45]. However, reasoning in the textual modality can only rely on single-pass image perception, which entails the risk of miss-

ing critical visual information [53], leading to recent methods [49, 61, 70] that attempt to expand the perceptual boundaries of VLMs by leveraging external tools. For instance, Hu et al. [12] grants VLMs the ability to use tools for manipulating images, enabling them to enhance reasoning in mathematical and visual tasks by drawing auxiliary lines. Huang et al. [15] finds that models trained with reinforcement learning (RL) can effectively use appropriate tools for complex multimodal reasoning. Groundlight AI [19] introduces GRPO training, teaching model to use zoom-in tools for reasoning, which improves the ability to recognize small objects in natural images. These studies demonstrate that visual reasoning with tool invocation can significantly enhance the reasoning abilities of VLMs in complex tasks. However, VLMs with tools [49, 70] mainly rely on OCR and object detection to construct supervised data, which limits their applicability to RS imagery that lacks textual elements and contains densely distributed small objects. In this work, we introduce a localization process with varying region scales and a Region-Guided reward to enhance the model’s capability for regional perception in RS images.

3. Method

3.1. Active Perception Oriented RS Dataset

Although recent studies [1, 56, 72] have emphasized the importance of benchmark datasets, resources specifically designed for high-resolution RS images remain scarce. Conventional RS VQA tasks typically operate on images of moderate resolution where objects are readily identifiable. In contrast, the UHR RS image, with its vast pixel space and sparse target distributions, poses a substantial challenge for direct global observation. To address these challenges, we

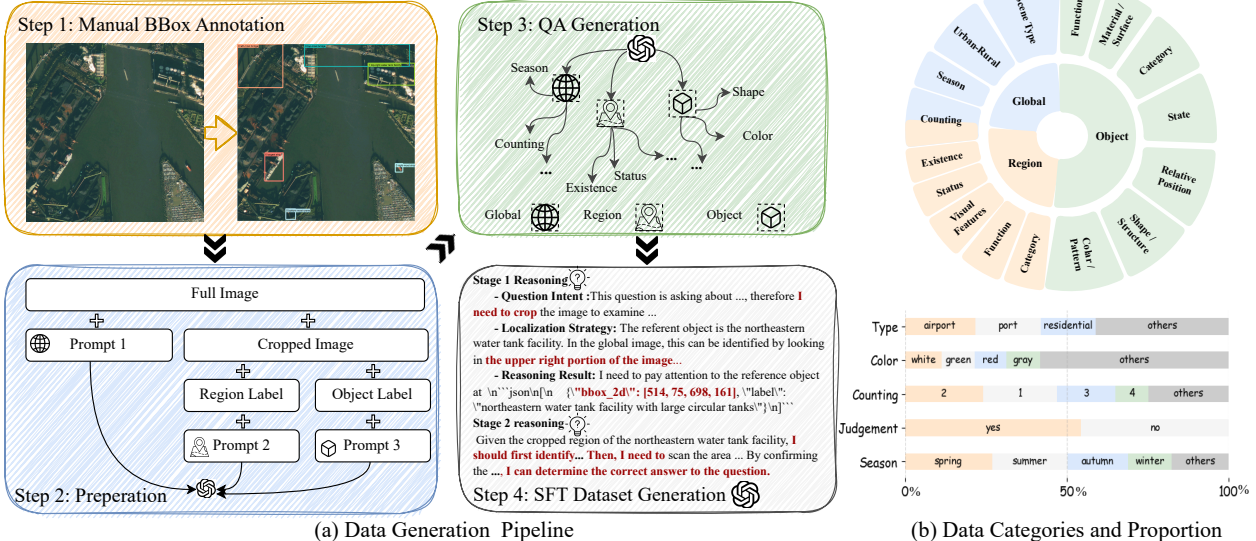


Figure 4. (a) Construction pipeline of our proposed LRS-GRO dataset, in which manual filtering and refinement are performed after Step 3. (b) The upper chart shows the 17 question types in the LRS-GRO dataset, whereas the lower chart shows the distribution of typical answer categories, demonstrating the dataset’s balance.

first propose a new benchmark task, Active Perception Oriented (APO) RS VQA, which requires models to actively locate, discriminate, and reason over fine-grained ROIs.

Definition 1 (Active Perception Oriented RS VQA). *The APO RS VQA task evaluates two core capabilities: (i) accurately answering questions about UHR RS images; (ii) identifying and attending to image regions that are relevant to the given question.*

This task involves an iterative active perception process and requires a comprehensive evaluation of a model’s semantic reasoning and spatial attention, assessing not only answer accuracy but also its active perception capability through ROI-based IoU.

3.1.1. Data Annotation Pipeline

To support this new task, we construct the LRS-GRO benchmark dataset using a novel semi-automatic annotation pipeline. Although LRS-VQA [41] has proposed a fully automated annotation method, it suffers from severe hallucinations of GPT when dealing with UHR RS images, making it unable to provide highly accurate BBox labels. To address this limitation, our process begins with manual annotation of BBoxes and their corresponding categories based on unique spatial characteristics (e.g., “the top-most bridge” and “the building with a yellow roof”). Moreover, we explicitly distinguish between region-level and object-level BBoxes, providing hierarchical labels that better capture the unique properties of RS images. The Region-level BBoxes focus on planned land areas composed of multiple objects with distinct semantic labels, such as airports, residential communities, and industrial zones, and thus contain

finer-grained compositional elements. In contrast, object-level BBoxes represent semantically homogeneous single objects, such as houses, airplanes, and ships.

Based on this, as shown in Fig. 4, we submit the entire image, cropped regions, and object-based enlarged crops to GPT-4o [44] to generate candidate Question–Answer (QA) pairs concerning attributes such as the target’s color, shape, and status. In total, 40k candidate QA pairs are generated, which are then manually filtered and refined to retain the highest-quality 13k pairs while maintaining answer balance. For constructing the SFT dataset, we also instruct GPT-4o to produce step-by-step reasoning processes that incorporate the cropping procedure.

3.1.2. Dataset Composition and Structure

Following LRS-VQA [41], our LRS-GRO benchmark is curated from imagery sourced from FAIR1M-1.0 [51], GLH-Bridge [26], and STAR [27]. The final dataset comprises 1,224 high-resolution images (4,000–5,000 px), 3,592 bounding boxes, and 13,245 questions. Among them, 1,000 samples with detailed step-by-step CoT annotations constitute the SFT dataset.

We define 17 major question categories organized into 3 hierarchical spatial levels:

- **Global:** Counting, Season, Urban–Rural, Scene Type
- **Region:** Counting, Existence, Status, Visual Features, Function, Category
- **Object:** Function, Material / Surface, Category, State, Relative Position, Shape / Structure, Color / Pattern

For region and object-level tasks, we provide the reference BBoxes to facilitate supervision and evaluation. This hierarchical structure is a key design choice, as it enables

Table 1. Comparison between RS vision-language benchmarks and our proposed dataset. ‘‘MME-R-W’’ denotes MME-Real-World [68]. The symbols \checkmark , \times , and \times represent manual, semi-automatic, and fully automatic annotation methods, respectively. Additional human verification is excluded.

Dataset	Avg. Resolution	Active Perception	VQA	
			Volume	Annotation
RSVQA [39]	512×512	N	111,134	\times
RSVQA-HR [39]	1,024×1,024	N	1,066,316	\times
VRSBench [25]	512×512	N	123,231	\times
RSIEval [13]	512×512	N	933	\checkmark
XLRS-Bench [55]	8,500×8,500	N	32,389	\checkmark
MME-R-W [68]	2000×1500	N	29429	\checkmark
LRS-VQA [41]	5,000×5,000	N	7333	\times
LRS-GRO	5,000×5,000	Y	13245	\times

models to adaptively determine whether cropping is necessary based on the question’s scope. Table 1 compares our dataset with existing benchmarks, underscoring its competitiveness in terms of resolution, scale, and its distinctive emphasis on active perception oriented VQA. More details are provided in Appendix 6.

3.2. ZoomEarth

Building on the LRS-GRO benchmark, we propose ZoomEarth, an adaptive cropping-zooming framework designed for active perception. The core idea is to mimic human-like visual search by first gaining a holistic understanding from a coarse overview, then actively focusing on specific regions for detailed inspection. As shown in Fig. 3, ZoomEarth first processes a downsampled version of the entire UHR image to understand the global context. Subsequently, for questions requiring fine-grained detail, the model actively predicts a BBox for the relevant ROI, which is then cropped from the original high-resolution image and re-fed into the model for a detailed perception. To learn this complex behavior, we employ a two-stage training strategy.

3.3. Training via SFT and RL

3.3.1. Stage 1: Supervised Fine-Tuning

We first initialize the model through SFT. In this stage, the Qwen2.5-VL-3B [4] model is fine-tuned on our SFT dataset. This process enables the model to focus on RS domain knowledge, learn to follow the predefined formats for tool invocation. In addition, it enables the model to build a fundamental capability to distinguish among task levels and their respective localization requirements.

3.3.2. Stage 2: Reinforcement Learning

While SFT teaches imitation, we employ reinforcement learning to build a more robust and generalizable decision-making policy. We adapt GRPO [46] for this stage. Its critic-free design offers significant memory efficiency, making it particularly well-suited for handling the long visual token sequences generated from UHR images.



Figure 5. Comparison between r_{IoU} and r_{R-G} .

3.3.3. Reward Design for Active Perception

A significant challenge in the RL stage is designing an effective reward function. Previous research [17, 38, 47] on VLMs trained with RL often employ IoU as the primary reward. However, due to the foundational weakness of VLMs on UHR images, predicted BBoxes often deviate significantly from the GT, causing the IoU reward to remain zero and provide no learning signal as shown in Fig. 5.

To address this issue, we propose the Region-Guided reward, specifically designed for UHR RS images. This reward is inspired by the observation that geographic objects often exhibit strong spatial associations, such as aircraft located near airport terminals. Therefore, we argue that predictions located near the GT BBox should be rewarded. The Region-Guided reward provides a dense, fine-grained guidance signal by rewarding predictions based on their distance to the GT, as formulated below:

$$r_{R-G} = \text{sigmoid}\left(\frac{\alpha}{\text{distance} + \epsilon}\right) \quad (1)$$

where α denotes the scale number related to the resolution and distance denotes the Euclidean distance between the center of the predicted BBox and the GT BBox center, and ϵ is a small constant to prevent numerical overflow. The final reward is defined as:

$$\text{Reward} = r_{IoU} + r_{R-G} + r_{\text{answer}} + \beta r_{\text{pattern}} \quad (2)$$

where r_{IoU} represents the IoU reward, the same as in VLM-R³ [17], r_{answer} is the normalized answer reward derived from word similarity [43], and r_{pattern} denotes the reward for the output format, assigned a value of 1 if correct and 0 if incorrect with the coefficient $\beta = 0.05$ controlling its influence. More explanations are provided in Appendix 7.

3.4. Toolkit for Downstream Tasks

Through the preceding training stages, the model acquires the capability to adaptively crop ROIs, ranging from region-level to object-level. This introduces the potential of a foundation model tailored for a wide spectrum of downstream tasks in the RS domain. Considering that directly performing tasks such as denoising and clouding removal on high-resolution global images incurs substantial computational costs and often yields limited practical benefits. As the framework shown in Fig. 6, our cropping-zooming

method enables the model to more efficiently focus on user-specified regions of interest in UHR RS. In a training-free manner, we integrate multiple advanced downstream models and design task-specific instructions to achieve adaptive tool invocation. Based on the proposed ZoomEarth model, we construct a scalable RS agent capable of performing functions including segmentation, denoising, clouding removal, and image editing.

4. Experiment

4.1. Settings and Implementation Details

4.1.1. Dataset

Training Data. We utilize the LRS-GRO dataset, which is split into approximately 3,500 samples for training and 10,000 samples for testing. In the first stage, we fine-tune the model on the SFT dataset, with tool-necessary and tool-unnecessary subsets in a 2:1 ratio. In the second stage, we fine-tune the model on 2,500 samples using RL to enhance its tool utilization and generalization ability.

Test Data. For evaluation, we assess model performance on the LRS-GRO test set and other datasets with resolutions exceeding 5000×5000 , including MME-Real-World [68], XLRS-Bench [55] and GeoLLava-8k [54].

4.1.2. Evaluation Metrics

Accuracy (Acc). We report Average Accuracy (Avg. Acc) for the VQA task across the aforementioned datasets. For LRS-GRO, the correctness of predictions is evaluated by measuring the semantic similarity between the predicted and ground-truth answers using WordNet [43], where a similarity score higher than 0.8 is regarded as correct[16, 41, 63]. For MME-Real-World [68], XLRS-Bench [55], we follow the evaluation setting provided by their respective datasets. Due to the lack of UHR RS datasets, we additionally incorporate the training dataset proposed by GeoLLava-8k[54] for testing, applying the same evaluation settings as that used for our proposed LRS-GRO dataset.

APO IoU. Standard VQA accuracy is insufficient as it does not evaluate how the model arrived at an answer. To measure the effectiveness of the localization step, we introduce the active perception oriented (APO) IoU. This metric is defined as the IoU between the predicted ROI bounding box and the ROI annotation. The APO IoU metric is applied to the region and object-level questions, as these tasks are designated to require tool invocation. A critical component of this evaluation is that if a model fails to generate a valid bounding box for a required task, its APO IoU for that sample is automatically set to 0. This directly penalizes failures in the active perception process, providing a comprehensive assessment of the model’s tool-use capability.

4.1.3. Implementation Details

All experiments are conducted on 8 NVIDIA A800 GPUs. During training, the images are processed at an input resolution of 512 pixels (before cropping). In the RL stage, the sampling temperature is set to 0.7, while for all evaluation experiments, the temperature is fixed at 0.01. Regarding the learning rate, it is set to 3e-5 in the SFT stage and 1e-7 in the RL stage. More details are provided in Appendix 8.

4.2. Main Results

Our model, built upon the Qwen2.5-VL 3B [4] architecture, consistently outperforms multiple baseline models on the LRS-GRO dataset, as shown in Table 2. Compared with InternVL3-8B that supports higher-resolution inputs, our model, with an initial input resolution of only 512, achieves substantial advantages in region-level and object-level tasks, improving accuracy by 1.53% and 4.00%. For global-level tasks that emphasize overall context rather than regional understanding, ZoomEarth is predictably lower than some larger models but still achieves a notable advantage over models of comparable size, such as Qwen2.5-VL-3B [4]. To ensure fairness, we adopt the Geochat [18] approach and fine-tuned its pre-trained weights on LRS-GRO using the same data. We observe that, despite Geochat having been trained on a large amount of additional RS data, ZoomEarth still demonstrates a significant advantage. Compared with the publicly available general-purpose tool-calling model VLM-R³ [17], our smaller model achieves a 3.59% performance gain. Moreover, our APO IoU reaches 34.39%, which is substantially higher than VLM-R³ [17]. This highlights the effectiveness and significance of our proposed dataset and training method for RS applications.

To evaluate the generalization capability of our model trained on the LRS-GRO dataset, we conduct zero-shot testing on three UHR RS datasets with all models evaluated under an input resolution of 1024. As shown in Table 3, compared with various VLMs from both general and RS domains, our model achieves SOTA performance on MME-RealWorld-RS [68], GeoLLava-8k [54], and XLRS-Bench [55]. Specifically, XLRS-Bench [55] provides pre-defined BBoxes in questions for region localization. Although this differs from our proposed framework that the model actively generates the BBox of the ROI, our method still demonstrates strong generalization ability.

4.3. Ablation Study

Ablation on cropping. To assess the effectiveness of the cropping–zooming tool, we conducted an ablation study by removing its application process. Specifically, we trained the model on the same dataset but required it to produce final answers without access to the cropped images. As shown in Table 4, the proposed active perception strategy yielded an average improvement of 4.39% across four

Table 2. Experimental results of various models on LRS-GRO. ‘‘Max Size’’ refers to the maximum resolution that the model can process as input. ‘‘method*’’ indicates we reproduce the SFT stage of existing methods using the same training data as ours. ‘‘-’’ denotes that the model lacks ROI localization outputs, making APO IoU evaluation impossible.

Leaderboard	LLM	Max Size	Global	Region	Object	Avg. Acc	APO IoU
LLaVA-OV-1.5 [3]	Qwen3-7B	$2,304 \times 2,304$	62.43	36.18	39.92	45.33	-
IXC-2.5 [65]	InternLM2-7B	$4,096 \times 4,096$	62.43	40.00	47.32	50.00	-
InternVL3 [59]	InternLM3-8B	3200×3200	71.60	44.58	47.80	53.67	-
Geochat [18]	Vicuna-1.5-7B	504×504	62.43	36.79	40.72	45.88	-
	Qwen2.5-7B	1024×1024	69.39	38.47	43.58	49.62	-
Qwen2.5-VL [4]		3333×3333	70.06	39.08	46.43	51.43	-
	Qwen2.5-3B	1024×1024	59.01	31.91	37.46	42.25	-
		3333×3333	58.90	31.76	38.66	42.83	-
VLM-R ³ [17] (w/ tools)	Qwen3-7B	512×512	69.72	44.83	37.40	50.17	19.93
Geochat*	Vicuna-1.5-7B	504×504	58.78	37.25	42.83	46.09	-
ZoomEarth (ours)	Qwen2.5-3B	512×512	63.09	46.11	51.80	53.76	34.39

Table 3. Zero-shot comparison of various models on MME-RealWorld-RS [68], XLRS-bench [55], GeoLLava-8k [54]. ‘‘-’’ indicates unavailable results due to potential data leakage risk from overlapping GeoLLava-8k and GeoChat training data.

Leaderboard	LLM	MME-realworld-RS	XLRS-bench	GeoLLava-8k	Avg. Acc
LLaVA-OV-1.5 [3]	Qwen3-7B	33.20	39.60	31.48	36.40
IXC-2.5 [65]	InternLM2-7B	36.12	31.50	36.20	34.61
InternVL3-8B [59]	InternLM3-8B	41.00	36.70	37.60	38.43
Geochat [18]	Vicuna-1.5-7B	28.62	22.03	-	-
Qwen2.5-VL [4]	Qwen2.5-3B	23.94	36.00	34.64	29.97
VLM-R ³ [17] (w/ tools)	Qwen3-7B	39.80	39.10	34.74	37.88
ZoomEarth (ours)	Qwen2.5-3B	44.10	40.20	38.61	40.97

Table 4. Ablation on cropping. ‘‘MME-R-W’’ means MME-RealWorld [68], XLRS refers to XLRS-bench [55]. ‘‘+ Cropping’’ indicates the incorporation of cropping–zooming functionalities.

Methods	LRS-GRO	MME-R-W	XLRS	GeoLLava-8k
ZoomEarth	51.10	42.10	30.00	34.30
+ Cropping	53.64 ^{±2.57}	44.10 ^{±2.00}	40.20 ^{±10.20}	38.61 ^{±4.31}

datasets. In addition, experiments conducted on other UHR RS datasets are under the zero-shot setting, which highlights the remarkable generalization ability of ZoomEarth.

Ablation on RL stage. To investigate the impact of the two-stage training strategy on enhancing the model’s tool reasoning capability, we removed the RL stage on the LRS-GRO dataset. An ablation study was then conducted on the MME-RealWorld-RS dataset to avoid overfitting to the training set (LRS-GRO). As shown in Table 5, after SFT alone, invoking the cropping tool unexpectedly resulted in a performance drop. This finding suggests that SFT-based imitation learning primarily aids the model in acquiring output formats, whereas RL is crucial to the model’s reasoning with tools and active perception capabilities.

Ablation on specific rewards. We conducted an ablation study on the LRS-GRO dataset to examine the effects of dif-

Table 5. Impact of RL on reasoning performance with tool usage.

Methods	Color	Count	Position	Overall
SFT	45.71	29.78	51.83	42.80
+ Cropping	45.40 _{±0.31}	27.90 _{±1.88}	49.58 _{±2.25}	41.30 _{±1.50}
RL	48.47	29.47	47.61	42.10
+ Cropping	49.69 _{±1.22}	31.66 _{±2.19}	50.14 _{±2.53}	44.10 _{±2.00}

Table 6. Ablation results for reward based on LRS-GRO.

r_{R-G}	r_{IOU}	Global	Region	Object	Avg. Acc
✗	✗	62.54	43.36	51.06	52.67
✓	✗	62.21	45.80	50.83	52.94
✗	✓	62.43	43.97	51.11	52.79
✓	✓	63.09	46.11	51.80	53.76

ferent rewards, focusing on the IOU reward and the Region-Guided reward. As shown in Table 6, removing the Region-Guided reward resulted in a performance drop of 0.97%, which is greater than the 0.82% drop observed when removing the IOU reward. This finding suggests that, for UHR RS images, the Region-Guided reward plays a more significant role than the IOU reward. Notably, compared with the setting without either IOU or Region-Guided rewards, adding the Region-Guided reward improved performance on region QA tasks by 2.44%, demonstrating stronger adaptability to region-level understanding questions.

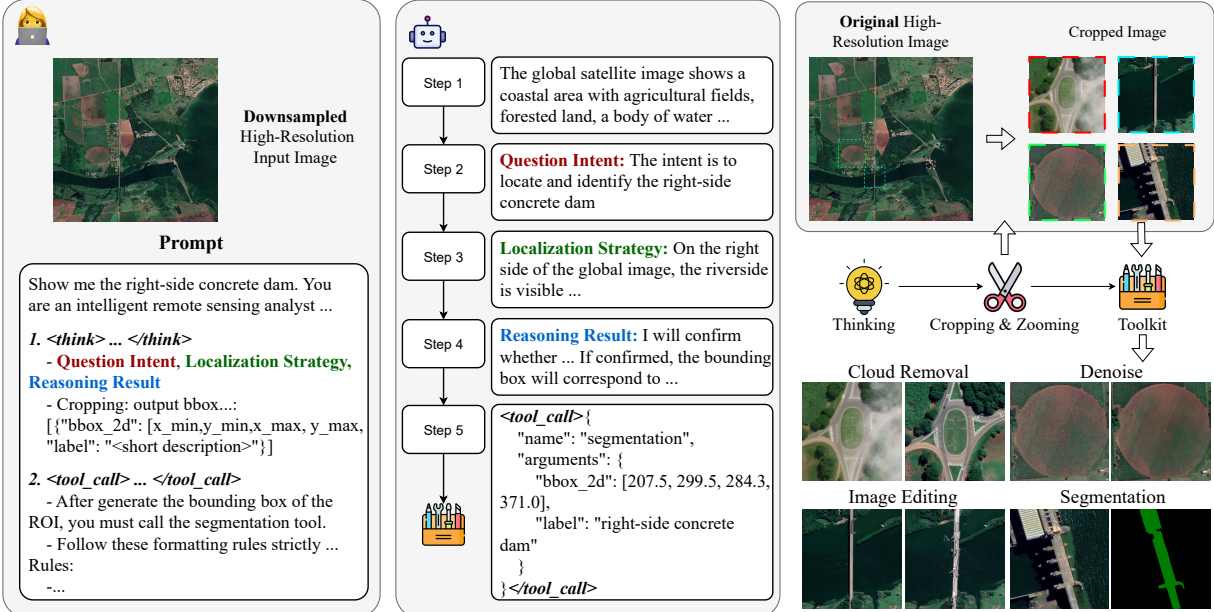


Figure 6. ZoomEarth inference pipeline with open tool invocation for cloud removal, denoising, image editing, and semantic segmentation. Due to the unavailability of suitable data for cloud removal, we simulated cloud-covered images using an image editing model [44].

Table 7. Ablation on inputting resolution. The model is evaluated during inference across various input resolutions under identical training data conditions.

Cropping	Max Size	Global	Region	Object	Avg. Acc	Speed (it/s)
✗	512×512	64.31	42.14	47.17	50.86	3.69
✗	1024×1024	63.76	41.37	48.32	51.16	3.50
✗	3333×3333	63.31	40.61	48.37	50.92	2.04
✓	512×512	64.53	44.43	51.06	53.43	2.38

Ablation on different resolution input. As shown in Table 7, we examine the performance differences of the model under varying input resolutions. The results indicate that, although increasing the resolution of input images provides more fine-grained visual information, it does not yield significant performance improvements, which means the model is easily disturbed by the redundant information introduced by a large number of visual tokens. However, after invoking the perception tool, the model still achieves a performance gain of over 2% at an input resolution of 512, suggesting that the our approach can effectively help the model overcome its performance bottleneck when processing high-resolution images and offers a significant speed advantage compared to 3333×3333 resolution input.

4.4. Unified Framework for Downstream Tasks

In practical applications, users typically focus on specific regions within high-resolution RS images, necessitating that the model possess the capability to autonomously identify and process the target regions. In our proposed approach, the model can identify ROIs using the cropping-zooming tool, and then performs subsequent processing reasoning. Through prompt-based instructions, we enable the model to invoke a broader set of tools and integrate spe-

cialized models from multiple domains, including cloud removal [37], denoising [29], image editing [33], and segmentation [22], as illustrated in Fig. 6. In implementation, we specify in the instructions that the model should output the BBox of the ROI within the tool invocation section, crop it from the original high-resolution image, and route it to the appropriate downstream model based on the determined tool name. Although our experiments are limited to a training-free setting, the results demonstrate that the model can adaptively select suitable tools from the toolkit according to the task requirements. The ZoomEarth model shows strong potential for UHR RS image processing and can be extended to a wide range of downstream tasks.

5. Conclusion

In this work, we introduce the concept of active perception to tackle the challenges of UHR RS VQA. We present LRS-GRO, a high-quality and diverse benchmark dataset spanning global, region, and object-level questions, enabling the stimulation and evaluation of active perception capabilities. Our proposed ZoomEarth framework adaptively calls the cropping-zooming tool to actively explore and extract fine-grained information from UHR images, guided by our proposed reward mechanism tailored to the distributional characteristics of RS scenes. Experimental results demonstrate competitive performance, strong generalization, and a scalable foundation for integrating downstream tasks. We anticipate that ZoomEarth will form the foundation for designing future autonomous RS agents, equipping them with the fundamental capability to actively seek information within complex, large-scale environments.

References

[1] Abduljaleel Adejumo, Faegheh Yeganli, Clifford Broni-bediako, Aoran Xiao, Naoto Yokoya, and Mennatullah Siam. A vision centric remote sensing benchmark. *arXiv preprint arXiv:2503.15816*, 2025. 3

[2] Saeed Ranjbar Alvar, Gursimran Singh, Mohammad Akbari, and Yong Zhang. Divprune: Diversity-based visual token pruning for large multimodal models. In *Proceedings of the IEEE/CVF Conference on Computer Vision and Pattern Recognition (CVPR)*, pages 9392–9401, 2025. 2

[3] Xiang An, Yin Xie, Kaicheng Yang, Wenkang Zhang, Xiuwei Zhao, Zheng Cheng, Yirui Wang, Songcen Xu, Changrui Chen, Chunsheng Wu, et al. Llava-onevision-1.5: Fully open framework for democratized multimodal training. *arXiv preprint arXiv:2509.23661*, 2025. 7

[4] Shuai Bai, Keqin Chen, Xuejing Liu, Jialin Wang, Wenbin Ge, Sibo Song, Kai Dang, Peng Wang, Shijie Wang, Jun Tang, et al. Qwen2.5-vl technical report. *arXiv preprint arXiv:2502.13923*, 2025. 3, 5, 6, 7

[5] Lucas Beyer, Andreas Steiner, André Susano Pinto, Alexander Kolesnikov, Xiao Wang, Daniel Salz, Maxim Neumann, Ibrahim Alabdulmohsin, Michael Tschannen, Emanuele Bugliarello, et al. Paligemma: A versatile 3b vlm for transfer. *arXiv preprint arXiv:2407.07726*, 2024. 1

[6] Yukang Chen, Wei Huang, Baifeng Shi, Qinghao Hu, Han-rong Ye, Ligeng Zhu, Zhijian Liu, Pavlo Molchanov, Jan Kautz, Xiaojuan Qi, et al. Scaling rl to long videos. *arXiv preprint arXiv:2507.07966*, 2025. 3

[7] Zhe Chen, Weiyun Wang, Yue Cao, Yangzhou Liu, Zhang-wei Gao, Erfei Cui, Jinguo Zhu, Shenglong Ye, Hao Tian, Zhaoyang Liu, et al. Expanding performance boundaries of open-source multimodal models with model, data, and test-time scaling. *arXiv preprint arXiv:2412.05271*, 2024. 3

[8] Xiaoyi Dong, Pan Zhang, Yuhang Zang, Yuhang Cao, Bin Wang, Linke Ouyang, Songyang Zhang, Haodong Duan, Wenwei Zhang, Yining Li, Hang Yan, Yang Gao, Zhe Chen, Xinyue Zhang, Wei Li, Jingwen Li, Wenhui Wang, Kai Chen, Conghui He, Xingcheng Zhang, Jifeng Dai, Yu Qiao, Dahua Lin, and Jiaqi Wang. Internlm-xcomposer2-4khd: A pioneering large vision-language model handling resolutions from 336 pixels to 4k hd. *arXiv preprint arXiv:2404.06512*, 2024. 2

[9] Hosam Elgendi, Ahmed Sharshar, Ahmed Aboeitta, Yasser Ashraf, and Mohsen Guizani. Geollava: Efficient fine-tuned vision-language models for temporal change detection in remote sensing. *arXiv preprint arXiv:2410.19552*, 2024. 3

[10] Jiawei Guo, Feifei Zhai, Pu Jian, Qianrun Wei, and Yu Zhou. Crop: Contextual region-oriented visual token pruning. *arXiv preprint arXiv:2505.21233*, 2025. 2

[11] Zonghao Guo, Ruyi Xu, Yuan Yao, Junbo Cui, Zanlin Ni, Chunjiang Ge, Tat-Seng Chua, Zhiyuan Liu, and Gao Huang. Llava-uhd: an lmm perceiving any aspect ratio and high-resolution images. In *European Conference on Computer Vision*, pages 390–406. Springer, 2024. 3

[12] Yushi Hu, Weijia Shi, Xingyu Fu, Dan Roth, Mari Ostendorf, Luke Zettlemoyer, Noah A Smith, and Ranjay Krishna. Visual sketchpad: Sketching as a visual chain of thought for multimodal language models. *Advances in Neural Information Processing Systems*, 37:139348–139379, 2024. 3

[13] Yuan Hu, Jianlong Yuan, Congcong Wen, Xiaonan Lu, Yu Liu, and Xiang Li. Rsgpt: A remote sensing vision language model and benchmark. *ISPRS Journal of Photogrammetry and Remote Sensing*, 224:272–286, 2025. 5

[14] Yuehao Huang, Liang Liu, Shuangming Lei, Yukai Ma, Hao Su, Jianbiao Mei, Pengxiang Zhao, Yaqing Gu, Yong Liu, and Jiajun Lv. Cogddn: A cognitive demand-driven navigation with decision optimization and dual-process thinking. In *Proceedings of the 33rd ACM International Conference on Multimedia*, page 5237–5246. ACM, 2025. 3

[15] Zeyi Huang, Yuyang Ji, Anirudh Sundara Rajan, Zefan Cai, Wen Xiao, Haohan Wang, Junjie Hu, and Yong Jae Lee. Visualtoolagent (vista): A reinforcement learning framework for visual tool selection. *arXiv preprint arXiv:2505.20289*, 2025. 3

[16] Drew A. Hudson and Christopher D. Manning. Gqa: A new dataset for real-world visual reasoning and compositional question answering. In *Proceedings of the IEEE/CVF Conference on Computer Vision and Pattern Recognition (CVPR)*, 2019. 6

[17] Chaoya Jiang, Yongrui Heng, Wei Ye, Han Yang, Haiyang Xu, Ming Yan, Ji Zhang, Fei Huang, and Shikun Zhang. Vlm-r³: Region recognition, reasoning, and refinement for enhanced multimodal chain-of-thought. *arXiv preprint arXiv:2505.16192*, 2025. 2, 5, 6, 7

[18] Kartik Kuckreja, Muhammad S. Danish, Muzammal Naseer, Abhijit Das, Salman Khan, and Fahad S. Khan. Geochat: Grounded large vision-language model for remote sensing. *The IEEE/CVF Conference on Computer Vision and Pattern Recognition*, 2024. 1, 3, 6, 7

[19] Sunil Kumar, Bowen Zhao, Leo Dirac, and Paulina Varshavskaya. Reinforcing vlms to use tools for detailed visual reasoning under resource constraints. *arXiv preprint arXiv:2506.14821*, 2025. 3

[20] Bozhou Li and Wentao Zhang. Id-align: Rope-conscious position remapping for dynamic high-resolution adaptation in vision-language models. *arXiv preprint arXiv:2505.21465*, 2025. 3

[21] Junyan Li, Delin Chen, Tianle Cai, Peihao Chen, Yining Hong, Zhenfang Chen, Yikang Shen, and Chuang Gan. Flex-attention for efficient high-resolution vision-language models. In *European Conference on Computer Vision*, pages 286–302. Springer, 2024. 3

[22] Kaiyu Li, Ruixun Liu, Xiangyong Cao, Xueru Bai, Feng Zhou, Deyu Meng, and Zhi Wang. Segearth-ov: Towards training-free open-vocabulary segmentation for remote sensing images. In *Proceedings of the Computer Vision and Pattern Recognition Conference*, pages 10545–10556, 2025. 8

[23] Kaiyu Li, Zepeng Xin, Li Pang, Chao Pang, Yupeng Deng, Jing Yao, Guisong Xia, Deyu Meng, Zhi Wang, and Xiangyong Cao. Segearth-r1: Geospatial pixel reasoning via large language model. *arXiv preprint arXiv:2504.09644*, 2025. 1

[24] Wentong Li, Yuqian Yuan, Jian Liu, Dongqi Tang, Song Wang, Jie Qin, Jianke Zhu, and Lei Zhang. Tokenpacker: Efficient visual projector for multimodal llm. *International Journal of Computer Vision*, pages 1–19, 2025. 1

[25] Xiang Li, Jian Ding, and Mohamed Elhoseiny. Vrsbench: A versatile vision-language benchmark dataset for remote sensing image understanding. *Advances in Neural Information Processing Systems*, 37:3229–3242, 2024. 5

[26] Yansheng Li, Junwei Luo, Yongjun Zhang, Yihua Tan, Jin-Gang Yu, and Song Bai. Learning to holistically detect bridges from large-size vhr remote sensing imagery. *IEEE Transactions on Pattern Analysis and Machine Intelligence*, 44(11):7778–7796, 2024. 3, 4

[27] Yansheng Li, Linlin Wang, Tingzhu Wang, Xue Yang, Junwei Luo, Qi Wang, Youming Deng, Wenbin Wang, Xian Sun, Haifeng Li, Bo Dang, Yongjun Zhang, Yi Yu, and Yan Junchi. Star: A first-ever dataset and a large-scale benchmark for scene graph generation in large-size satellite imagery. *IEEE Transactions on Pattern Analysis and Machine Intelligence*, 2024. 4

[28] Yu Li, Jin Jiang, Jianhua Zhu, Shuai Peng, Baole Wei, Yuxuan Zhou, and Liangcai Gao. Uni-mumer: Unified multi-task fine-tuning of vision-language model for handwritten mathematical expression recognition. *arXiv preprint arXiv:2505.23566*, 2025. 3

[29] Yanyi Li, Xi Zhang, Yisi Luo, and Deyu Meng. Deep rank-one tensor functional factorization for multi-dimensional data recovery. *Proceedings of the AAAI Conference on Artificial Intelligence*, 39(17):18539–18547, 2025. 8

[30] Zihang Li and Haowen Hou. Visualrvkv-hd and uhd: Advancing high-resolution processing for visual language models. *arXiv preprint arXiv:2410.11665*, 2024. 3

[31] Zhang Li, Biao Yang, Qiang Liu, Zhiyin Ma, Shuo Zhang, Jingxu Yang, Yabo Sun, Yuliang Liu, and Xiang Bai. Monkey: Image resolution and text label are important things for large multi-modal models. In *proceedings of the IEEE/CVF conference on computer vision and pattern recognition*, pages 26763–26773, 2024. 3

[32] Yuxuan Liang, Xu Li, Xiaolei Chen, Yi Zheng, Haotian Chen, Bin Li, and Xiangyang Xue. Pyramid token pruning for high-resolution large vision-language models via region, token, and instruction-guided importance. *arXiv preprint arXiv:2509.15704*, 2025. 3

[33] Chenyang Liu, Keyan Chen, Rui Zhao, Zhengxia Zou, and Zhenwei Shi. Text2earth: Unlocking text-driven remote sensing image generation with a global-scale dataset and a foundation model. *arXiv preprint arXiv:2501.00895*, 2025. 8

[34] Haotian Liu, Chunyuan Li, Qingyang Wu, and Yong Jae Lee. Visual instruction tuning. *Advances in neural information processing systems*, 36:34892–34916, 2023. 1

[35] Haotian Liu, Chunyuan Li, Yuheng Li, and Yong Jae Lee. Improved baselines with visual instruction tuning. In *Proceedings of the IEEE/CVF Conference on Computer Vision and Pattern Recognition (CVPR)*, pages 26296–26306, 2024. 1

[36] Haotian Liu, Chunyuan Li, Yuheng Li, Bo Li, Yuanhan Zhang, Sheng Shen, and Yong Jae Lee. Llava-next: Improved reasoning, ocr, and world knowledge, january 2024. URL <https://llava-vl.github.io/blog/2024-01-30-llava-next>, 1(8), 2024. 1

[37] Yi Liu, Wengen Li, Jihong Guan, Shuigeng Zhou, and Yichao Zhang. Effective cloud removal for remote sensing images by an improved mean-reverting denoising model with elucidated design space. In *Proceedings of the Computer Vision and Pattern Recognition Conference*, pages 17851–17861, 2025. 8

[38] Ziyu Liu, Zeyi Sun, Yuhang Zang, Xiaoyi Dong, Yuhang Cao, Haodong Duan, Dahua Lin, and Jiaqi Wang. Visual-rft: Visual reinforcement fine-tuning. *arXiv preprint arXiv:2503.01785*, 2025. 3, 5

[39] Sylvain Lobry, Diego Marcos, Jesse Murray, and Devis Tuia. Rsvqa: Visual question answering for remote sensing data. *IEEE Transactions on Geoscience and Remote Sensing*, 58(12):8555–8566, 2020. 5

[40] Gen Luo, Yiyi Zhou, Yuxin Zhang, Xiawu Zheng, Xiaoshuai Sun, and Rongrong Ji. Feast your eyes: Mixture-of-resolution adaptation for multimodal large language models. *arXiv preprint arXiv:2403.03003*, 2024. 3

[41] Junwei Luo, Yingying Zhang, Xue Yang, Kang Wu, Qi Zhu, Lei Liang, Jingdong Chen, and Yansheng Li. When large vision-language model meets large remote sensing imagery: Coarse-to-fine text-guided token pruning. *arXiv preprint arXiv:2503.07588*, 2025. 1, 2, 3, 4, 5, 6

[42] Utkarsh Mall, Cheng Perng Phoo, Meilin Kelsey Liu, Carl Vondrick, Bharath Hariharan, and Kavita Bala. Remote sensing vision-language foundation models without annotations via ground remote alignment. In *The Twelfth International Conference on Learning Representations*, 2024. 1

[43] George A. Miller. Wordnet: a lexical database for english. *Commun. ACM*, 38(11):39–41, 1995. 5, 6

[44] OpenAI, Aaron Hurst, Adam Lerer, and et al. Gpt-4o system card. *arXiv preprint arXiv:2410.21276*, 2024. 4, 8

[45] Hao Shao, Shengju Qian, Han Xiao, Guanglu Song, Zhuofan Zong, Letian Wang, Yu Liu, and Hongsheng Li. Visual cot: Advancing multi-modal language models with a comprehensive dataset and benchmark for chain-of-thought reasoning. *Advances in Neural Information Processing Systems*, 37:8612–8642, 2024. 3

[46] Zhihong Shao, Peiyi Wang, Qihao Zhu, Runxin Xu, Junxiao Song, Xiao Bi, Haowei Zhang, Mingchuan Zhang, YK Li, Yang Wu, et al. Deepseekmath: Pushing the limits of mathematical reasoning in open language models. *arXiv preprint arXiv:2402.03300*, 2024. 2, 5

[47] Haozhan Shen, Peng Liu, Jingcheng Li, Chunxin Fang, Yibo Ma, Jiajia Liao, Qiaoli Shen, Zilun Zhang, Kangjia Zhao, Qianqian Zhang, et al. Vlm-r1: A stable and generalizable r1-style large vision-language model. *arXiv preprint arXiv:2504.07615*, 2025. 5

[48] Baifeng Shi, Boyi Li, Han Cai, Yao Lu, Sifei Liu, Marco Pavone, Jan Kautz, Song Han, Trevor Darrell, Pavlo Molchanov, et al. Scaling vision pre-training to 4k resolution. In *Proceedings of the Computer Vision and Pattern Recognition Conference*, pages 9631–9640, 2025. 3

[49] Alex Su, Haozhe Wang, Weiming Ren, Fangzhen Lin, and Wenhui Chen. Pixel reasoner: Incentivizing pixel-space reasoning with curiosity-driven reinforcement learning. *arXiv preprint arXiv:2505.15966*, 2025. 3

[50] Haopeng Sun, Yingwei Zhang, Lumin Xu, Sheng Jin, and Yiqiang Chen. Ultra-high resolution segmentation via boundary-enhanced patch-merging transformer. *arXiv preprint arXiv:2412.10181*, 2024. 3

[51] Xian Sun, Peijin Wang, Zhiyuan Yan, Feng Xu, Ruiping Wang, Wenhui Diao, Jin Chen, Jihao Li, Yingchao Feng, Tao Xu, et al. Fair1m: A benchmark dataset for fine-grained object recognition in high-resolution remote sensing imagery. *ISPRS Journal of Photogrammetry and Remote Sensing*, 184:116–130, 2022. 4

[52] Gemini Team, Rohan Anil, Sebastian Borgeaud, Jean-Baptiste Alayrac, Jiahui Yu, Radu Soricut, Johan Schalkwyk, Andrew M Dai, Anja Hauth, Katie Millican, et al. Gemini: a family of highly capable multimodal models. *arXiv preprint arXiv:2312.11805*, 2023. 1

[53] Shengbang Tong, Zhuang Liu, Yuexiang Zhai, Yi Ma, Yann LeCun, and Saining Xie. Eyes wide shut? exploring the visual shortcomings of multimodal llms. In *Proceedings of the IEEE/CVF Conference on Computer Vision and Pattern Recognition*, pages 9568–9578, 2024. 3

[54] Fengxiang Wang, Mingshuo Chen, Yueying Li, Di Wang, Haotian Wang, Zonghao Guo, Zefan Wang, Boqi Shan, Long Lan, Yulin Wang, et al. Geollava-8k: Scaling remote-sensing multimodal large language models to 8k resolution. *arXiv preprint arXiv:2505.21375*, 2025. 1, 6, 7

[55] Fengxiang Wang, Hongzhen Wang, Zonghao Guo, Di Wang, Yulin Wang, Mingshuo Chen, Qiang Ma, Long Lan, Wenjing Yang, Jing Zhang, et al. Xlrs-bench: Could your multimodal llms understand extremely large ultra-high-resolution remote sensing imagery? In *Proceedings of the Computer Vision and Pattern Recognition Conference*, pages 14325–14336, 2025. 5, 6, 7

[56] Junjue Wang, Zhuo Zheng, Zihang Chen, Ailong Ma, and Yanfei Zhong. Earthvqa: Towards queryable earth via relational reasoning-based remote sensing visual question answering. In *Proceedings of the AAAI conference on artificial intelligence*, pages 5481–5489, 2024. 3

[57] Jiacong Wang, Zijian Kang, Haochen Wang, Haiyong Jiang, Jiawen Li, Bohong Wu, Ya Wang, Jiao Ran, Xiao Liang, Chao Feng, et al. Vgr: Visual grounded reasoning. *arXiv preprint arXiv:2506.11991*, 2025. 2

[58] Peng Wang, Shuai Bai, Sinan Tan, Shijie Wang, Zhihao Fan, Jinze Bai, Keqin Chen, Xuejing Liu, Jialin Wang, Wenbin Ge, et al. Qwen2-vl: Enhancing vision-language model’s perception of the world at any resolution. *arXiv preprint arXiv:2409.12191*, 2024. 1

[59] Weiyun Wang, Zhangwei Gao, Lixin Gu, Hengjun Pu, Long Cui, Xinguang Wei, Zhaoyang Liu, Linglin Jing, Shenglong Ye, Jie Shao, et al. Internvl3. 5: Advancing open-source multimodal models in versatility, reasoning, and efficiency. *arXiv preprint arXiv:2508.18265*, 2025. 7

[60] Xingxing Weng, Chao Pang, and Gui-Song Xia. Vision-language modeling meets remote sensing: Models, datasets, and perspectives. *IEEE Geoscience and Remote Sensing Magazine*, 13(3):276–323, 2025. 1

[61] Penghao Wu and Saining Xie. V*: Guided visual search as a core mechanism in multimodal llms. *arXiv preprint arXiv:2312.14135*, 2023. 3

[62] Zhiyu Wu, Xiaokang Chen, Zizheng Pan, Xingchao Liu, Wen Liu, Damai Dai, Huazuo Gao, Yiyang Ma, Chengyue Wu, Bingxuan Wang, et al. Deepseek-vl2: Mixture-of-experts vision-language models for advanced multimodal understanding. *arXiv preprint arXiv:2412.10302*, 2024. 3

[63] Junbin Xiao, Xindi Shang, Angela Yao, and Tat-Seng Chua. Next-qa: Next phase of question-answering to explaining temporal actions. In *Proceedings of the IEEE/CVF Conference on Computer Vision and Pattern Recognition (CVPR)*, pages 9777–9786, 2021. 6

[64] Chen Yi and Shan LianLei. A global-local cross-attention network for ultra-high resolution remote sensing image semantic segmentation. *arXiv preprint arXiv:2506.19406*, 2025. 3

[65] Pan Zhang, Xiaoyi Dong, Yuhang Zang, Yuhang Cao, Rui Qian, Lin Chen, Qipeng Guo, Haodong Duan, Bin Wang, Linke Ouyang, et al. Internlm-xcomposer-2.5: A versatile large vision language model supporting long-contextual input and output. *arXiv preprint arXiv:2407.03320*, 2024. 7

[66] Wei Zhang, Miaoxin Cai, Tong Zhang, Yin Zhuang, Jun Li, and Xuerui Mao. Earthmarker: A visual prompting multi-modal large language model for remote sensing. *IEEE Transactions on Geoscience and Remote Sensing*, 63:1–19, 2025. 3

[67] Yusen Zhang, Wenliang Zheng, Aashrith Madasu, Peng Shi, Ryo Kamoi, Hao Zhou, Zhuoyang Zou, Shu Zhao, Sarkar Snigdha Sarathi Das, Vipul Gupta, et al. Hrscene: How far are vlms from effective high-resolution image understanding? *arXiv preprint arXiv:2504.18406*, 2025. 3

[68] Yi-Fan Zhang, Huanyu Zhang, Haochen Tian, Chaoyou Fu, Shuangqing Zhang, Junfei Wu, Feng Li, Kun Wang, Qingsong Wen, Zhang Zhang, et al. Mme-realworld: Could your multimodal llm challenge high-resolution real-world scenarios that are difficult for humans? *arXiv preprint arXiv:2408.13257*, 2024. 5, 6, 7

[69] Yuzhong Zhao, Feng Liu, Yue Liu, Mingxiang Liao, Chen Gong, Qixiang Ye, and Fang Wan. Dynrefer: Delving into region-level multimodal tasks via dynamic resolution. In *Proceedings of the Computer Vision and Pattern Recognition Conference*, pages 24742–24752, 2025. 2

[70] Ziwei Zheng, Michael Yang, Jack Hong, Chenxiao Zhao, Guohai Xu, Le Yang, Chao Shen, and Xing Yu. Deep-eyes: Incentivizing “thinking with images” via reinforcement learning. *arXiv preprint arXiv:2505.14362*, 2025. 3

[71] Xirui Zhou, Lianlei Shan, and Xiaolin Gui. Dynrl-vlm: Enhancing autonomous driving perception with dynamic resolution vision-language models. *arXiv preprint arXiv:2503.11265*, 2025. 1

[72] Xing Zi, Jinghao Xiao, Yunxiao Shi, Xian Tao, Jun Li, Ali Braytee, and Mukesh Prasad. Rsvlm-qa: A benchmark dataset for remote sensing vision language model-based question answering. In *Proceedings of the 33rd ACM International Conference on Multimedia*, page 12905–12911, New York, NY, USA, 2025. Association for Computing Machinery. 3

ZoomEarth: Active Perception for Ultra-High-Resolution Geospatial Vision-Language Tasks

Supplementary Material

6. LRS-GRO Dataset

6.1. Data Generation Details

The dataset construction process involves three distinct settings: **object-level**, **region-level**, and **global-level** VQA with their corresponding CoT annotations. For each setting, both the input to the annotation model (GPT-4o) and the expected output format are defined explicitly.

6.2. Region-level and Object-level VQA.

For non-global cases, human annotators first manually select ROIs in the image by drawing bounding boxes. Each ROI is further categorized as either:

- **Region:** a spatially extended area containing multiple objects or structures, where the cropped image is taken directly from the bounding box.
- **Object:** a single target object of interest, where the bounding box is expanded before cropping to provide additional surrounding context.

For each selected ROI, the following information is passed to GPT-4o:

1. A downsampled version of the full image (for global context).
2. A high-resolution cropped image derived from the bounding box (region: direct crop; object: expanded crop).
3. The human-provided label describing the object's or region's position and type.
4. The bounding box coordinates.

Then GPT-4o will generate Question-Answer pairs based on prompts shown in Appendix 6.2.

Dataset Annotation Prompt of Object Questions

You are an expert dataset annotator for an *Object-level Visual Question Answering (VQA) dataset*.

You will be provided with:

1. A downsampled full image showing the global context.
2. A high-resolution cropped image centered on the target object (ROI).
3. A bounding box for the object: `{item.get('bbox')}`.
4. A short human-provided label describing the object's **global position and type**: `{item.get('label')}`.

Your tasks:

1. **Refine the label** into a clear and specific English name for the object, preserving its spatial description. Examples:
 - “top-most sports field” → “top-most tennis court”
 - “central building” → “central white office building”
2. **Generate several high-quality, image-dependent question-answer pairs** about this object:
 - Use the refined label **explicitly** (no pronouns like “this object” or “it”).
 - Be **visually grounded** — cannot be answered by common sense alone.
 - Require looking at the provided images to answer.
 - Avoid trivial or universal facts (e.g., airplane has wings, grass is green).

Object-level Question Categories:

1. **Object category refinement** — Make the label more specific based on visual cues. Examples:
 - “Is the top-most sports field a tennis court or a basketball court?”
 - “Is the left-side bridge designed for vehicles or pedestrians?”
2. **Object color / pattern** — Non-obvious or detailed color info. Examples:
 - “What color is the roof of the central building?”
 - “Is the top-right ship mainly white or blue?”
 - “Does the top-most tennis court have a green or red surface?”
3. **Object shape / structure** — Shape or structural details. Examples:
 - “What is the shape of the top-most building’s roof?”
 - “Is the left-side bridge straight or curved?”
 - “Is the bottom-right ship narrow or wide?”
4. **Object function / usage** — Purpose or role inferred from context. Examples:
 - “What is the function of the central rectangular building?”
 - “Is the left-side bridge used for vehicles or trains?”

5. **Object state / motion / activity** — Current condition or movement. Examples:
 - “Is the right-most vehicle moving or parked?”
 - “Is the top-left airplane taking off or landing?”
 - “Is the central crane operating or idle?”
6. **Object material / surface** — Visible material cues. Examples:
 - “Is the left-side bridge made of metal or concrete?”
 - “Does the roof of the central building appear metallic or tiled?”
7. **Object relative position / context** — Spatial relations to nearby elements. Examples:
 - “What is located beneath the top-most bridge?”
 - “Is there water below the bottom bridge?”
 - “What is on the right side of the central building?”

Guidelines:

- Use the refined label directly in all questions (no pronouns).
- Ensure each question is visually discriminative — answerable only by observing the images.
- Keep answers concise: “yes”, “no”, “concrete”, “curved”, “green”, “train”, “parked”, “water”.
- Each question must include:
 - “category” — one of the seven categories above.
 - “higher_level” — one of:
 - * “perception” — visual recognition (color, shape, count)
 - * “localization” — spatial position or relative location
 - * “attribute” — appearance or material properties
 - * “function” — role or purpose
 - * “reasoning” — inferred or dynamic states

Output format:

```
{
  "label": "top-most tennis court",
  "qa_pairs": [
    {
      "question": "Is the top-most sports field a tennis court or a basketball court?",
      "answer": "tennis court",
      "category": "Object category refinement",
      "higher_level": "attribute"
    },
  ]
}
```

```
{
  "question": "Does the top-most tennis court have a green or red surface?",
  "answer": "green",
  "category": "Object color / pattern",
  "higher_level": "perception"
},
{
  "question": "Is the top-most tennis court surrounded by fences?",
  "answer": "yes",
  "category": "Object shape / structure",
  "higher_level": "reasoning"
},
{
  "question": "What is located next to the top-most tennis court?",
  "answer": "parking lot",
  "category": "Object relative position / context",
  "higher_level": "localization"
}
]
```

Dataset Annotation Prompt of Region Questions

You are an expert dataset annotator for a Visual Question Answering (VQA) dataset.

You will be given:

1. A downsampled full image.
2. A high-resolution cropped image of the region of interest (ROI).
3. A bounding box representing the ROI: `{item.get('bbox')}`.
4. A short human-provided description of the ROI: `{item.get('label')}`.

Your task:

- Refine the label to make it a **precise and natural English name** for this region (e.g., “central bridge area”, “left-most parking lot”, “top-most construction site”).
- Generate several **diverse question–answer pairs** about the ROI, following the categories below.

Question categories (choose those applicable to the region):

1. **Counting** — Ask about the **number** of visible

objects. Examples:

- “How many vehicles are on the bridge?”
- “How many ships are docked near the pier?”

2. **Object existence** — Ask if certain objects are **present** in the ROI. Examples:

- “Is there a ship passing under the bridge?”
- “Are there any cars in the parking lot?”
- “Is any airplane on the runway?”

3. **Region status** — Ask about **activity, usage, or condition** of the region. Examples:

- “Is the bridge busy or empty?”
- “Is the construction site still active?”
- “Are there ships currently docking at the port?”
- “Is the road under construction or in use?”

4. **Object category** — Ask about the **types of main objects** found in the ROI. Examples:

- “What types of vehicles are in the parking lot?”
- “What kind of boats are docked at the pier?”

5. **Region function** — Ask about the **purpose or role** of the region. Examples:

- “What is this area mainly used for?”
- “What is the function of this rectangular region?”

6. **Other visual features** — Ask about **appearance, color, or shape** of the region or its objects. Examples:

- “Are most buildings in this area red-roofed?”
- “What is the overall shape of this region?”
- “Is the area circular or rectangular?”

Output requirements:

- Only ask **reasonable** questions that can be answered directly from the provided images.
- Provide concise answers (one word or short phrase). Examples: “yes”, “no”, “asphalt”, “empty”, “circular”, “urban”, “in use”.
- Each question must include:
 - “category”: one of the six above.
 - “higher_level”: one of these abstract reasoning levels:
 - * “perception” — direct visual recognition
 - * “localization” — position or spatial relation
 - * “attribute” — appearance or measurable quality
 - * “function” — purpose or role
 - * “reasoning” — requires inference or contextual understanding

Output format:

```
{
  "label": "top-most bridge area",
  "qa_pairs": [
    {
      "question": "How many vehicles are on the bridge?",  

      "answer": "3",  

      "category": "Counting",  

      "higher_level": "perception"
    },
    {
      "question": "Is the bridge currently in use?",  

      "answer": "yes",  

      "category": "Region status",  

      "higher_level": "reasoning"
    },
    {
      "question": "Are there ships passing under the bridge?",  

      "answer": "no",  

      "category": "Object existence",  

      "higher_level": "perception"
    },
    {
      "question": "What type of vehicles are visible on the bridge?",  

      "answer": "cars",  

      "category": "Object category",  

      "higher_level": "attribute"
    },
    {
      "question": "What is the main function of this bridge area?",  

      "answer": "transportation",  

      "category": "Region function",  

      "higher_level": "function"
    }
  ]
}
```

6.3. Global-level VQA

For global-level questions, the full high-resolution satellite image is directly provided to GPT-4o, together with a task-specific prompt (see Appendix 6.3). The model is instructed to generate scene-level, visually grounded question–answer pairs that require holistic understanding of the image, such as scene type, counting of large-scale objects, or seasonal inference.

Dataset Annotation Prompt of Global Questions

You are an expert dataset annotator for a Visual Question Answering (VQA) task focusing on *global-level understanding* of high-resolution remote sensing images.

You will be provided with:

1. A full high-resolution image covering the entire scene.

Your task: Generate several **high-quality, globally grounded question–answer pairs** in English about the image.

Requirements for each question:

- **Scene-level**, not object-level.
- **Visually grounded** — answerable purely by looking at the image.
- **Specific and unique** — avoid vague or overly general questions.
- Generate only if the image clearly supports it; otherwise, output an empty list.

Possible question types (use only when appropriate):

- **Counting** — e.g., “How many airplanes are visible in the image?”
- **Urban–Rural** — e.g., “Does this image mainly depict an urban or rural area?”
- **Scene Type** — e.g., “What is the main type of area shown — airport, residential, or farmland?”
- **Season** — e.g., “What season does the scene appear to be?”

Higher-level reasoning categories:

- perception
- localization
- attribute
- function
- reasoning

Output format (strict JSON):

```
{  
  "qa_pairs": [  
    {  
      "question": "How many airplanes  
      are visible in the image?",  
      "answer": "3",  
      "category": "Counting",  
      "higher_level": "perception",  
      "justification": "Airplanes are  
      distinct and countable  
      across the visible runways."  
    },  
    {  
    }
```

```
      "question": "What is the main  
      type of area shown in this  
      image airport, residential,  
      or farmland?",  
      "answer": "airport",  
      "category": "Scene Type",  
      "higher_level": "reasoning",  
      "justification": "The image  
      shows large runways and  
      parked airplanes typical of  
      an airport."  
    }  
  ]  
}
```

6.4. SFT Dataset Annotation

In order to train the model to master both the step-by-step reasoning process and the standardized tool invocation format for answering questions, we employed GPT-4o to generate annotations using a two-stage reasoning–cropping–reasoning CoT paradigm, as defined in the prompt provided in Appendix 6.4.

Reasoning-based remote sensing VQA Annotation Prompt

You are an intelligent remote sensing analyst.
Your task is to generate reasoning-based annotations for Visual Question Answering (VQA) using satellite imagery.

I will provide:

- A global satellite image (downsampled for efficiency)
- The bounding box $[x_{\min}, y_{\min}, x_{\max}, y_{\max}]$ of the **reference object** mentioned in the question
- A natural language question referring to the image
- The ground truth answer

Important:

- The reference bounding box corresponds to the **referent object** in the question (e.g., if the question asks “What is the structure parallel and closest to the bridge?”, the reference bbox is for the bridge).
- The final target answer is derived **by reasoning relative to this referent object**.
- The global image should only be used for context and to explain how one would locate the referent region.
- The final answer must be derived **by analyzing the cropped region corresponding to the referent object**.

ent and its surroundings.

When writing `<stage_1_reasoning>`, follow these rules:

- At the very start, always begin with: “*This question is asking about <short intent>, therefore I need to crop the image to examine the surroundings of the mentioned target.*”
- **Localization Strategy:** Describe the approximate location of the referent object in natural language (e.g., “the bottom-most long bridge across the river”). Do not output exact coordinates.
- **Reasoning Result:** First output exactly: “*I need to pay attention to the reference object at*” Then output the bounding box in JSON format on the next line:

```
[  
  {"bbox_2d": [x_min, y_min, x_max  
  , y_max], "label": "<short  
  description of the referent  
  object>"}  
]
```

No additional explanation in this section.

Output must strictly follow this structure:

```
<global> - Provide a brief but  
  informative description of the  
  global satellite image (e.g., main  
  structures, spatial layout). </  
  global>  
  
<stage_1_reasoning>  
Question Intent: Identify the type of  
  question being asked (e.g., object  
  category, count, color, spatial  
  relation, etc.), and determine  
  what visual information is needed  
  to answer it.  
  
Localization Strategy: Parse the  
  question to identify the referent  
  object (e.g., bridge, river,  
  building cluster). Translate the  
  description into a visual query  
  and locate it in the global image  
  using semantic cues (shape, size,  
  color, spatial arrangement).  
Summarize the approximate location  
  of the referent in natural  
  language.  
  
Reasoning Result:  
I need to pay attention to the  
  reference object at
```

```
[JSON bounding box]  
</stage_1_reasoning>
```

```
<stage_2_reasoning>
```

Given the cropped region of the referent object, explain how to reason about the final target answer. Specify what visual features or spatial relations should be observed. Clearly connect the reasoning steps from the referent to the final answer.

```
</stage_2_reasoning>
```

Constraints:

- Do not reveal the final answer in `<stage_1_reasoning>`.
- The `<global>` description must be neutral and avoid giving away the answer.
- The `<stage_2_reasoning>` must directly connect the referent to the final target.

Input:

```
Question: {result["question"]}  
Ground Truth Answer: {result["  
  ground_truth"]}  
Reference Bounding box: {[int(x /  
  scale) for x in hbox]}}
```

6.5. Data Refinement

Using GPT-4o, we initially generated over 40,000 question-answer pairs. However, several issues were observed during quality inspection. For binary (True/False) questions, the model exhibited a tendency to generate questions whose correct answer was “Yes,” while rarely producing negative cases. For multiple-choice questions, certain answer options were disproportionately favored, for example, “cement” in material-related questions or “summer” in season-related questions. To address these biases, we manually removed redundant or overly similar questions and supplemented the dataset with additional questions to balance the distribution of answer options. Furthermore, some model-generated outputs contained factual or logical errors, which were corrected through manual revision. The refinement process was carried out by six annotators, each contributing over ten hours of work. Compared to fully manual annotation of tens of thousands of questions, our proposed semi-automatic data annotation pipeline significantly reduced the annotation workload while maintaining both label accuracy and distributional balance.

Configuration	VQA	
	SFT	GRPO
Training component	Full	Full
Learning rate	3e-5	1e-7
Warmup step	500	50
Weight decay	0.01	0.01
Batch size	4	32
α	-	200
β	-	0.05
γ	-	0.04
Optimizer	AdamW	
Dataset	LRS-GRO/sft	LRS-GRO/rl
Training epoch	1	1

Table 8. Experimental configurations and hyperparameters for SFT and GRPO training. In the GRPO objective, α controls the Region-Guided reward, β scales the pattern reward in the overall reward formulation, and γ regulates the KL-divergence penalty.

6.6. Dataset Visualization

As shown in Figs 8, 9, 10 and 11, we visualize a subset of QA pairs from the LRS-GRO dataset, covering multiple representative geographic landscapes such as airports, factories, ports, bridges, and rural areas. The LRS-GRO dataset provides abundant question–answer pairs and precise bounding box annotations for the global, regional, and object levels.

6.7. Comparison with LRS-VQA Dataset

As illustrated in Figs 12, 13, 14 and 15, the LRS-VQA dataset innovatively introduced a GPT-based automated annotation pipeline, offering a novel approach to data labeling. However, due to noticeable hallucinations when GPT processes high-resolution imagery, as illustrated in the figure, incorrect labels may provide the model with misleading rewards during training, thereby hindering convergence. Following the annotation paradigm of LRS-VQA, we further refined and proposed the LRS-GRO dataset. Through meticulous manual annotation and verification, we provide a high-resolution RS image dataset with precise labels.

7. Training Details

Table 8 summarizes the experimental configurations and hyperparameters used for the ZoomEarth under the SFT and GRPO training settings.

For a detailed implementation of GRPO, the objective function is defined as follows:

$$\mathcal{J}_{\text{GRPO}}(\theta) = \mathbb{E} \left[q \sim P_{\text{sft}}(Q), \{o_i\}_{i=1}^G \sim \pi_{\theta_{\text{old}}}(O|q) \right] \frac{1}{G} \sum_{i=1}^G \frac{1}{|o_i|} \sum_{t=1}^{|o_i|} \left[\hat{A}_{i,t}^* - \gamma \mathbb{D}_{\text{KL}}[\pi_{\theta} \parallel \pi_{\theta_{\text{ref}}}] \right] \quad (3)$$

where $P_{\text{sft}}(Q)$ denotes the distribution of queries sampled

from the supervised fine-tuning dataset, and $\pi_{\theta}(O|q)$ represents the current policy parameterized by θ , which generates output sequences conditioned on the query q . $\hat{A}_{i,t}^*$ denotes the clipped advantage reweighted by importance sampling, and $\mathbb{D}_{\text{KL}}[\pi_{\theta} \parallel \pi_{\theta_{\text{ref}}}]$ represents an unbiased estimator of the KL divergence. G denotes the number of samples per group, and $|o_i|$ indicates the length of each trajectory. Specifically, γ is set to 0.04, and G is set to 4.

$$\mathbb{D}_{\text{KL}}[\pi_{\theta} \parallel \pi_{\theta_{\text{ref}}}] = \frac{\pi_{\theta_{\text{ref}}}(o_{i,t}|q, o_{i,< t})}{\pi_{\theta}(o_{i,t}|q, o_{i,< t})} - \log \frac{\pi_{\theta_{\text{ref}}}(o_{i,t}|q, o_{i,< t})}{\pi_{\theta}(o_{i,t}|q, o_{i,< t})} - 1 \quad (4)$$

$$\hat{A}_{i,t}^* = \min \left[\frac{\pi_{\theta}(o_{i,t}|q, o_{i,< t})}{\pi_{\theta_{\text{old}}}(o_{i,t}|q, o_{i,< t})} \hat{A}_{i,t}, \text{clip} \left(\frac{\pi_{\theta}(o_{i,t}|q, o_{i,< t})}{\pi_{\theta_{\text{old}}}(o_{i,t}|q, o_{i,< t})}, 1 - \epsilon, 1 + \epsilon \right) \hat{A}_{i,t} \right] \quad (5)$$

$$\hat{A}_{i,t} = \frac{r_i - \text{mean}(r)}{\text{std}(r)} \quad (6)$$

The detailed reward components are defined as follows:

$$r_{IoU} = \begin{cases} IOU, & \text{if match} \\ 0, & \text{otherwise} \end{cases} \quad (7)$$

$$r_{R-G} = \text{sigmoid} \left(\frac{\alpha}{distance + \epsilon} \right) \quad (8)$$

$$r_{\text{answer}} = \begin{cases} 1, & \text{if similarity} > 0.8 \\ similarity, & \text{otherwise} \end{cases} \quad (9)$$

$$r_{\text{pattern}} = \begin{cases} 1, & \text{if match the pattern} \\ 0, & \text{otherwise} \end{cases} \quad (10)$$

$$r = r_{IoU} + r_{R-G} + r_{\text{answer}} + \beta r_{\text{pattern}} \quad (11)$$

Specifically, we set ϵ to 0.2. The parameter β is used to constrain the model outputs to adhere to the predefined format, thereby preventing training collapse. Our experiments show that when $\beta < 0.05$, e.g., $\beta = 0.01$, it fails to take effect and may lead to potential training collapse. Under the premise of stable output formatting, more than 99% of the r_{pattern} rewards are equal to 1, and thus increasing β has no impact on the overall reward after normalization. Therefore, we set $\beta = 0.05$ in our final configuration.

Finally, the model updates its parameters by performing gradient ascent on the GRPO objective:

$$\theta \leftarrow \theta + \eta \nabla_{\theta} \mathcal{J}_{\text{GRPO}}(\theta) \quad (12)$$

where η denotes the learning rate, which is set to 1×10^{-7} in our experiments.

To equip the model with the ability to perform chain-of-thought reasoning in this specific scenario, we applied instruction tuning during both the SFT and RL stages, and used the same instruction prompts during inference to elicit the reasoning capability acquired during training. Specifically, our instruction is as follows:

Instruction Used in Training and Evaluation

You are an intelligent remote sensing analyst.

Given a natural language question about a satellite image, generate a structured reasoning answer as follows:

1. `<think> ... </think>`
 - Provide a neutral one-sentence description of the whole image scene.
 - Cropping task:
“This question is asking about `<short intent>`, therefore I need to crop the image to examine the surroundings of the mentioned target.”
 - Non-cropping task:
“This question is asking about `<short intent>`, therefore I need to analyze the entire image without cropping.”
 - Include:
 - **Question Intent:** describe the type of question (object category, spatial relation, count, etc.) and the visual information needed.
 - **Localization Strategy:**
 - * Cropping: approximate referent object location in natural language (no coordinates).
 - * Non-cropping: strategy to detect all relevant objects across the entire image.
 - **Reasoning Result:**
 - * **Cropping:** output exactly one JSON-formatted bbox for the referent, for example:

```
[{"bbox_2d": [x_min, y_min, x_max, y_max], "label": "<short description>"}]
```

- * **Non-cropping:** summarize how detected objects will be used to produce the count or answer.

2. `<think> ... </think>` (only when the cropped image is provided)
 - Explain step-by-step how to reason from the referent (or detected objects) to the final answer.

3. `<answer> ... </answer>`

- Provide your final answer as a single word or short phrase.

Rules:

- Always return exactly one `<answer>` block.
- For tasks that need cropping:
 - Provide the bounding box of the object of interest in the first `<think>` block.
 - After the cropped image is given, generate another `<think>` block to derive the answer.
 - Also include a bounding box in the `<stage_2_reasoning>` block when required.
- If unsure about localization, make a best reasonable guess — never state uncertainty.

8. Inference Details

8.1. Visualization of the Reasoning Process

As illustrated in the Figs 16, 17, 18 and 19, the reasoning process of ZoomEarth is structured into several sequential stages to ensure both global comprehension and precise localization.

1. **Global Description:** The process begins with a comprehensive global analysis of the input image. This stage aims to establish an overall semantic understanding of the scene, enabling the model to capture contextual relationships and spatial configurations before focusing on specific regions.
2. **Question Intent Identification:** Following global perception, the model analyzes the user’s query to determine its underlying intent. This step isolates the core informational demand, ensuring that subsequent reasoning is aligned with the question’s focus.
3. **ROI Localization Strategy:** Based on the global understanding and the identified question intent, the model performs targeted localization reasoning. This involves determining the spatial regions most relevant to the query and representing them via bounding boxes.
4. **Tool Calling:** Once ROIs are identified, the model invokes appropriate tools to process the localized areas. This stage is referred to as *secondary perception*, as the model re-examines the image after cropping and zooming the identified regions. The objective is to increase resolution and focus on fine-grained visual details that may be lost in the global view.
5. **Stage 2 Reasoning:** The refined, high-resolution inputs derived from the localized regions are then used for a second stage of reasoning. This stage integrates global context with localized detail to produce the final answer, ensuring accuracy and relevance to the original query.

This multi-stage process is designed to balance broad contextual awareness with precise visual focus. By first establishing a global understanding and then iteratively narrowing attention to relevant regions, the ZoomEarth model mitigates the risk of missing context while maximizing the accuracy of localized inference.

8.2. Comparison with Other Models

Many methods have been proposed to address high-resolution image processing, as shown in Fig. 7. Techniques such as dynamic resolution and visual token pruning have become mainstream. Dynamic resolution methods first pad the image to an integer multiple of small patches and then split it into a sequence of small patches. This allows the model to handle high-resolution images but does not reduce the number of visual tokens, so a large number of tokens still need to be processed. Visual token pruning removes tokens with low information content or redundant information according to manually defined rules, reducing the number of visual tokens and enabling the model to handle high-resolution images. However, this approach relies on hand-crafted rules and has limited generalizability.

Our proposed method first feeds a downsampled low-resolution image into the model. The model then identifies ROIs and calls the cropping-zooming tool to obtain detailed information for these areas. This reduces the total number of visual tokens while preserving fine-grained details in the ROIs.

As illustrated in the Figs 20, 21 and 22, for questions at the region-level or object-level, general VLMs often produce incorrect answers due to limited visual resolution or hallucinations. Although VLMR³ is capable of performing secondary perception, its training methodology is not well-suited for high-resolution RS imagery, rendering it ineffective in this context. In contrast, our proposed ZoomEarth model can accurately localize the region of interest and perform reasoning based on the secondary perception of that region, thereby producing correct answers.

8.3. Evaluation of APO IoU

During inference, the model only outputs the region of interest or target, while the answer is often located in the adjacent area outside the ROIs. Therefore, we expand the predicted bounding box to a size of 512 and crop it from the original image. Accordingly, the APO IoU is computed after enlarging both the ground-truth and predicted bounding boxes to a fixed size of 512.

9. Downstream Tasks

9.1. Downstream Instructions

ZoomEarth can autonomously invoke external tools to perform downstream tasks such as cloud removal, denoising,

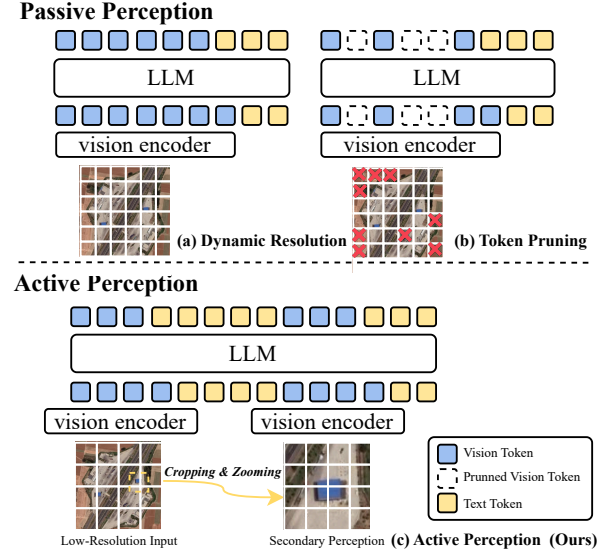


Figure 7. Detailed comparison between passive perception and our proposed active perception method.

segmentation, and image editing without additional training. By simply modifying the instruction, the model can be endowed with the ability to utilize these tools effectively. Specifically, the instructions we used in downstream tasks are:

Instruction Used for Downstream tasks

You are an intelligent remote sensing analyst.

Given a natural language question about a satellite image, generate a structured reasoning answer as follows:

1. <think> ... </think>
 - Provide a neutral one-sentence description of the whole image scene.
 - Cropping task: “This question is asking about <short intent>, therefore I need to crop the image to examine the surroundings of the mentioned target.”
 - Non-cropping task: “This question is asking about <short intent>, therefore I need to analyze the entire image without cropping.”
 - Include:
 - **Question Intent:** describe the type of question (object category, spatial relation, count, etc.) and needed visual information.
 - **Localization Strategy:**
 - * Cropping: approximate referent object location in natural language (no coordinates).
 - * Non-cropping: strategy to detect all relevant objects.

– **Reasoning Result:**

- * **Cropping:** output exactly one JSON-formatted bbox for the referent:

```
[{"bbox_2d": [x_min, y_min,
             x_max, y_max],
 "label": "<short description
             >"}]
```

- * **Non-cropping:** summarize how detected objects will be used to produce the count.

2. <tool_call> ... </tool_call>
 - After generating the bounding box of the ROI, you must call the tools below.
 - Follow these formatting rules strictly:
 - You must output exactly one <tool_call> block.
 - The content inside must be a valid JSON object in the following format:

```
<tool_call>
{
  "name": "tool_name",
  "arguments": {
    "arg1": arg1
  }
}</tool_call>
```

- Available tools:

* **Cloud removal:**

```
"name": "cloud_removal",
"arguments": {
  "bbox_2d": [x_min, y_min,
              x_max, y_max]
}
```

* **Segmentation:**

```
"name": "segmentation",
"arguments": {
  "bbox_2d": [x_min, y_min,
              x_max, y_max],
  "objects": [obj1, obj2]
}
```

* **Denoise:**

```
"name": "denoise",
"arguments": {
  "bbox_2d": [x_min, y_min,
              x_max, y_max]
}
```

* **Image editing:**

```
"name": "image_editing",
```

```
"arguments": {
  "bbox_2d": [x_min, y_min,
              x_max, y_max],
  "description": "Remove the
                 tree"
}
```

- Do not include any reasoning or comments outside the <tool_call> block.
- If localization is uncertain, make a best-guess bounding box.
- Ensure that the JSON inside <tool_call> is valid and machine-readable.

3. Example:

```
<tool_call>
{
  "name": "cloud_removal",
  "arguments": {
    "bbox_2d": [120.5, 230.1, 6
                40.3, 880.2]
  }
}</tool_call>
```

9.2. Downstream Examples

Below are examples of ZoomEarth's response to downstream task's instructions.

Cloud removal

Prompt: Show me the bottom-most blue-roofed building. And then remove the cloud over it using tools. + downstream instruction

<think>
The global satellite image shows a large industrial facility surrounded by forested areas and some urban infrastructure. The layout includes multiple rectangular buildings, open storage yards, and adjacent access roads and rail lines. There are also some construction zones and partially visible structures, along with surrounding natural land cover patterns.

Question Intent: This question is asking about identifying the position of a specific blue-roofed

building at the bottom-most part of the image, therefore I need to crop the image to examine the surroundings of the mentioned target.

Localization Strategy: The referent object is described as a blue-roofed building located at the bottom-most part of the scene. In the global image, these blue-roofed buildings appear as dark-colored rectangular structures with light-colored roofs, positioned towards the lower end of the industrial complex, near the edge of forested areas and road networks.

Reasoning Result: First, I locate the bottom-most blue-roofed building by identifying the lowest rectangular structure with a lighter roof within the industrial complex. Its position is at the southernmost part of the scene, directly adjacent to forested terrain, and slightly above a cluster of smaller buildings. Then, I crop the image to focus solely on this building to perform further operations.

```
</think>
<tool_call>
{
  "name": "cloud_removal",
  "arguments": {
    "bbox_2d": [379.5, 400.5,
                393.0, 411.5]
  }
}</tool_call>
```

regions. The layout includes long rectangular structures arranged in a linear fashion, some connected by overpasses or elevated roads, and several smaller buildings scattered around the complex.

Question Intent: This question is asking about identifying a specific blue-roofed building at the bottommost position in the facility, therefore I need to crop the image to examine the surroundings of the mentioned target.

Localization Strategy: The referent object is the bottom-most blue-roofed building. In the global image, this corresponds to a small rectangular structure with a bright blue roof located toward the lower right corner of the facility, near the edge of the wooded area.

Reasoning Result:
I need to pay attention to the bottom-right section of the global image where a small, distinct blue-roofed structure can be seen. This is positioned at the lower end of the main facility area, above open storage lots, and in close proximity to the forested terrain. The blue roof distinguishes it from other nearby buildings or structures.

```
</think>
<tool_call>
{
  "name": "segmentation",
  "arguments": {
    "bbox_2d": [340.5, 395.5, 398.0, 461.0],
    "objects": ["bottom-most blue-roofed building"]
  }
}</tool_call>
```

Segmentation

Prompt: Show me the bottom-most blue-roofed building. And then segment it using tools. + downstream instruction

```
<think>
The global satellite image shows a
large industrial facility with
multiple buildings, open storage
areas, and adjacent forested
```

Denoising

Prompt: Show me the bottom-most blue-roofed building. And then denoise the area around it using tools. + downstream instruction

```
<think>
The global satellite image shows a
large industrial facility with
multiple warehouse-like buildings,
large storage yards, and elevated
conveyor systems. The site is
surrounded by hilly terrain with
open fields and some scattered
clusters of buildings. Road
networks and bridges connect
different parts of the complex,
indicating active transportation
links.
```

Question Intent: This question is asking about identifying the bottom-most blue-roofed building after locating the referent, therefore I need to crop the image to examine the surroundings of the mentioned target.

Localization Strategy: The referent object is described as the bottom-most blue-roofed building. In the global image, blue-roofed structures stand out due to their bright coloration against the lighter-toned roofs and surrounding terrain. The lowest building among them would be the southernmost one in the facility layout, which is distinctly located at the bottom of the image. I can locate it by scanning along the southern edge of the facility and identifying the lowest blue-roofed structure.

Reasoning Result:

I need to pay attention to the referent object at

```
```json
[
 {"bbox_2d": [347.5, 398.5, 398.0,
 449.0], "label": "bottom-most
 blue-roofed building"}
]
```
</think>
<tool_call>
```

```
{
  "name": "denoise",
  "arguments": {
    "bbox_2d": [347.5, 398.5, 398.0,
    449.0]
  }
}</think>
```

Image editing

Prompt: Show me the bottom-most blue-roofed building. And then paint its roof red using tools. + downstream instruction

```
<think> The global satellite image
shows a large industrial facility
with multiple rectangular
buildings arranged in a grid-like
pattern across several plots.
There are large paved areas, some
with clearings, and surrounding
the facility are open land and
vegetation. Roads connect
different sections of the complex
within and around the periphery.
```

Question Intent: This question is asking about identifying and then visually changing the roof color of a specific blue-roofed building, therefore I need to crop the image to examine the surroundings of the mentioned target.

Localization Strategy: The referent object is described by its roof color - specifically blue. In the global image, blue roofs can be identified among the large rectangular buildings occupying the lower right section of the facility. These buildings have distinctively colored roofs, making them stand out from other structures due to their hue. The blue-roofed building in question is located toward the bottom-right corner of the facility, near the edge where the paved area meets the vegetation.

Reasoning Result:

I need to pay attention to the reference object at

```
```json
[
 {"bbox_2d": [357.5, 409.0, 399.5,
 446.0], "label": "bottom-most
 blue-roofed building"}
]
```
</think>
<tool_call>
{
    "name": "image_editing",
    "arguments": {
        "bbox_2d": [357.5, 409.0, 399.
            5, 446.0],
        "description": "Paint the roof
            of the bottom-most blue-
            roofed building red using
            appropriate tools."
    }
}
</think>
```



Figure 8. The visualization of examples from LRS-GRO dataset.



Figure 9. The visualization of examples from LRS-GRO dataset.



Figure 10. The visualization of examples from LRS-GRO dataset.



Figure 11. The visualization of examples from LRS-GRO dataset.



Figure 12. Comparison Between LRS-GRO and LRSVQA.



Figure 13. Comparison between LRS-GRO and LRSVQA.

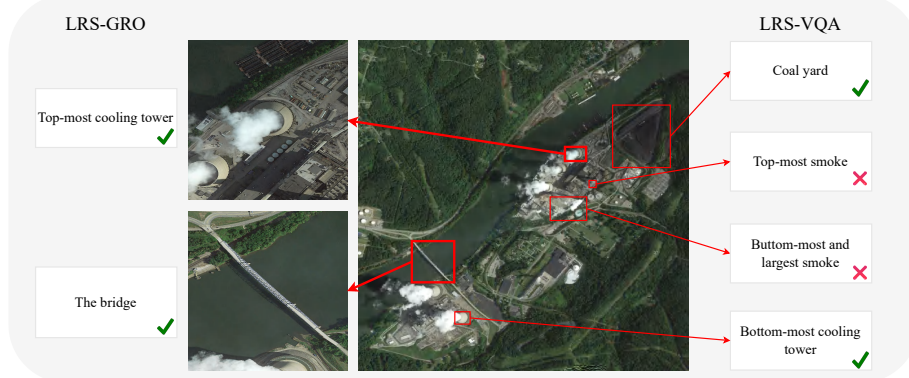
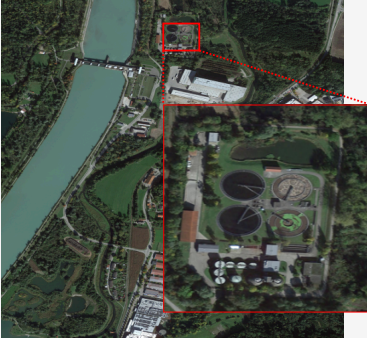


Figure 14. Comparison between LRS-GRO and LRSVQA.



Figure 15. Comparison between LRS-GRO and LRSVQA.



How many large circular tanks are visible in the top-center wastewater treatment plant?

Global Description <think> The global satellite image shows a coastal area with a river running along the left side, surrounded by forested land on both sides. There are several industrial facilities, including power plants and wastewater treatment plants, located inland near the river...

Question Intent This question is asking about counting the number of large circular tanks in a specific wastewater treatment plant, therefore I need to **crop the image** to examine the surroundings of the mentioned target.

Localization Strategy The referent object is the **"top-center wastewater treatment plant."** In the global image, this is identifiable as a large industrial facility with multiple rectangular buildings and open storage areas, situated inland near the river. It is positioned roughly in the upper central portion of the image...

Tool Calling **Reasoning Result** I need to pay attention to the reference object at: `[{"bbox_2d": [209.5, 34.0, 268.0, 67.0], "label": "top-center wastewater treatment plant"}]` <think>

Stage 2 Reasoning <think> To determine the number of large circular tanks in the cropped region, I should closely examine the facility's layout and identify any circular structures... By counting each distinct circular tank, I can arrive at the final answer. <think> <answer></answer>

Figure 16. Reasoning process visualization of ZoomEarth.



Is the bottom-most large container ship's bow rounded or pointed?

Global Description <think> The global satellite image shows a coastal port facility with multiple docks, piers, and container storage areas. There are several large cargo ships docked along the waterfront, surrounded by green vegetation inland...

Question Intent This question is asking about the shape of the bow of a specific large container ship, therefore I need to **crop the image** to examine the surroundings of the mentioned target.

Localization Strategy The referent object is the bottom-most large container ship in the image. It can be identified by its size, position at the lower end of the dock area, and its distinctive container stacks on deck. In the global image, this ship is located near the southernmost part of the port...

Tool Calling **Reasoning Result** I need to pay attention to the reference object at: `[{"bbox_2d": [209.5, 340.0, 228.0, 360.0], "label": "bottom-most large container ship"}]` <think>

Stage 2 Reasoning <think> To determine whether the bow is rounded or pointed, I should closely examine the cropped region containing the referent ship. The bow refers to the front section of the vessel, which can be visually assessed by looking at the shape of the upper hull... By focusing on the bow area in the cropped image, I can infer the correct classification based on its visual characteristics. <think> <answer>rounded</answer>

Figure 17. Reasoning process visualization of ZoomEarth.



Is the top-right blue factory buildings industrial area currently active?

Global Description <think> The global satellite image shows a large airport complex with multiple runways, taxiways, and terminal buildings. Surrounding the airport are various industrial zones, warehouses, and some undeveloped land....

Question Intent This question is asking about the operational status of a specific industrial facility, therefore I need to **crop the image** to examine the surroundings of the mentioned target.

Localization Strategy The referent object is the **"top-right blue factory buildings industrial area."** In the global image, this can be identified by looking at the upper right section where there are large rectangular blue-roofed structures situated near open land and road networks...

Tool Calling **Reasoning Result** I need to pay attention to the reference object at: `[{"bbox_2d": [149.5, 10.0, 511.5, 50.0], "label": "top-right blue factory buildings industrial area"}]` <think>

Stage 2 Reasoning <think> To determine if the top-right blue factory buildings are currently active, I should **examine the cropped region** for signs of ongoing operations such as visible activity, machinery, or equipment... By analyzing these visual cues in the cropped image, I can infer the operational status of the industrial area. <think> <answer>yes</answer>

Figure 18. Reasoning process visualization of ZoomEarth.



How many large bridges crossing the river are visible in the image?

Global description <think> The global satellite image shows a large river running diagonally across the frame, with two distinct landmasses on either side. On the left side, there is a densely built-up urban area with numerous buildings, roads, and some industrial zones...

Question Intent This question is asking about counting the number of large bridges crossing the river, therefore I need to **analyze the entire image without cropping**.

Localization Strategy To locate large bridges, I will look for long, wide structures spanning across the river, often with multiple lanes for vehicles and sometimes featuring roadways or rail tracks. These bridges typically have a consistent width along their span and may connect two distinct landmasses...

Reasoning result Once all potential large bridges are identified, I will verify their size and connection status... Once all potential large bridges are identified, I will verify their size and connection status...

Final answer By focusing only on the main, continuous structure, I conclude the count based on its presence and direct connection across the river. <think> <answer>1</answer>

Figure 19. Reasoning process visualization of ZoomEarth.

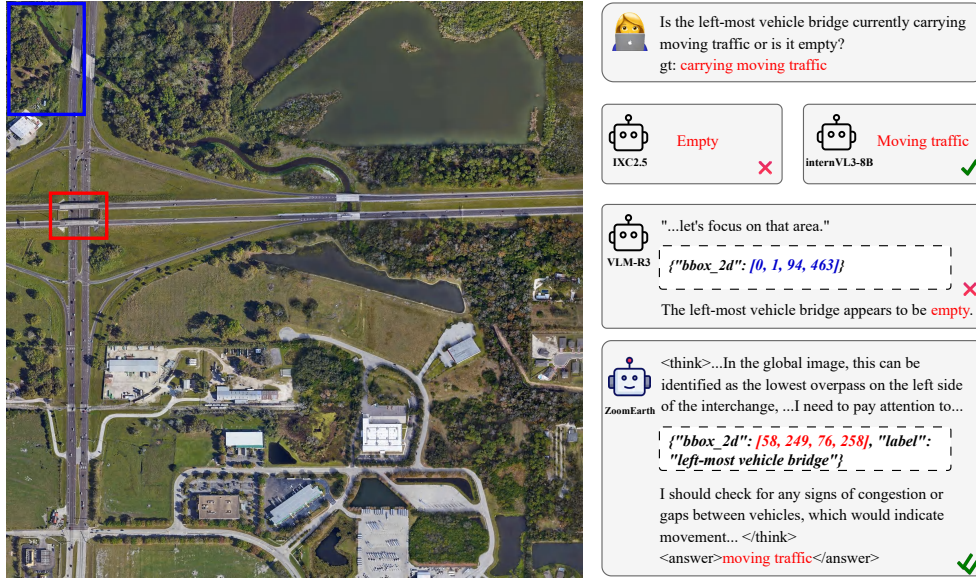


Figure 20. The comparison of the answer between different models.



Figure 21. The comparison of the answer between different models.

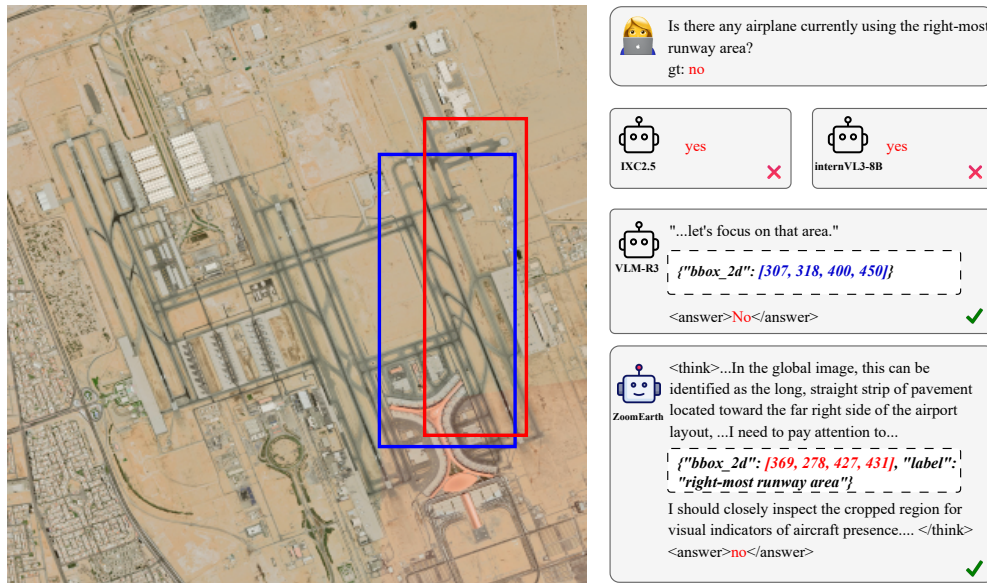


Figure 22. The comparison of the answer between different models.